Generalised homogenisation procedures for granular materials — **Source link** ↗

Elena Pasternak, Hans Muhlhaus

Institutions: University of Western Australia, University of Queensland

Topics: Discrete system, Finite difference, Wave propagation, Finite difference method and Characteristic length

Related papers:

- Théorie des corps déformables

- Dispersion and wave propagation in discrete and continuous models for granular materials

- Micro-structure in linear elasticity

- A continuum model for periodic two-dimensional block structures

- Second gradient of strain and surface-tension in linear elasticity

GENERALISED HOMOGENISATION PROCEDURES FOR GRANULAR MATERIALS

E. Pasternak[1] and H.-B. Mühlhaus[2]

[1]Department of Civil and Resource Engineering, The University of Western Australia, 35 Stirling Hwy, Crawley, WA 6009, Australia; email: elena@civil.uwa.edu.au

[2]Department of Earth Sciences, The University of Queensland, St Lucia, QLD 4072, Australia, email: muhlhaus@quakes.uq.edu.au

ABSTRACT

Engineering materials are generally non-homogeneous, yet standard continuum descriptions of such materials are admissible, provided that the size of the non-homogeneities is much smaller than the characteristic length of the deformation pattern. If this is not the case, either the individual non-homogeneities have to be described explicitly or the range of applicability of the continuum concept is extended by including additional variables or degrees of freedom. In the paper we model the discrete nature of granular materials in the simplest possible way by means of finite-difference equations. The difference equations may be homogenised in two ways: the simplest approach is to replace the finite differences by the corresponding Taylor expansions. This leads to a Cosserat continuum theory. A more sophisticated strategy is to homogenise the equations by means of a discrete Fourier transformation. The result is a Kunin-type non-local theory. In the following we analyse these theories by considering a model consisting of independent periodic 1D chains of solid spheres connected by shear translational and rotational springs. It is found that the Cosserat theory offers a healthy balance between accuracy and simplicity. Kunin's integral homogenisation theory leads to a non-local Cosserat continuum description that yields an exact solution, but does not offer any real simplification in the solution of the model equations as compared to the original discrete system. The rotational degree of freedom affects the phenomenology of wave propagation considerably. When the rotation is suppressed, only one type of wave, *viz.* a shear wave, exists. When the restriction on particle rotation is relaxed, the velocity of this wave decreases and another, high velocity wave arises.

Key words: Non-standard continua, Homogenisation, Rotational degrees of freedom, Cosserat continuum, Non-local continuum, Wave propagation

1. INTRODUCTION. COMPARATIVE ANALYSIS OF NON-STANDARD CONTINUA APPROACH TO MODELLING MATERIALS WITH MICROSTRUCTURE

1.1. Non-standard continua

There are cases when the classical continuum mechanics approach is insufficient to model adequately materials with microstructure. In particular, microstructure cannot be ignored when one considers layered material, especially when the layers can slide, blocky structures, granular media, cracked media. The consideration of microstructure is necessary when the size of redistribution of an external load is comparable with the microstructure size or if the stress gradients at intergranular contact points (finite contact area, modelled as a contact point) of grains have to be be taken into account.

Naturally, there are different approaches (or combinations thereof) to take microstructural effects into account. Each approach results into different types of standard or non-standard continua.

The first step in the adaptation or extension of a standard continuum theory to granular materials is the introduction of rotational degrees of freedom in addition to the conventional translational ones (if for instance the spin of particles is important). This leads to gradient or higher-order gradient theories (when further degrees of freedom have to be included as well), resulting in the introduction of additional strain measures and the correspondent stress tensors.

While the need for independent rotational DOF's (Cosserat type theories, eg Cosserat [1]; Nowacki [2]) is quite easy to understand in the context of granular and layered materials, further increase of DOF requires more explanations. Mindlin [3] based his reasoning on the simultaneous consideration of macro- and micro- displacements within a volume element.

In the spirit of Mindlin's discussion we consider a macro-volume, i.e. the domain occupied by a body, and choose a Cartesian coordinate system $x_1x_2x_3$ (see Figure 1). Let *P* be an arbitrary point of a body, the position of the point in the macro-volume being determined by the macro-coordinates x_i. The macro-motion of this point can be described by the macro-displacement vector $\boldsymbol{u}(x_i)$ and macro-rotation vector $\boldsymbol{\varphi}$=1/2rot$\boldsymbol{u}$. According to the conventional continuum mechanics, the deformation measures at this point are the components of the macro-distortion tensor $u_{i,j}$, the symmetric part of which gives usual components of a macro-

strain tensor $\varepsilon_{ij}=1/2(u_{i,j}+u_{j,i})$. The antisymmetric part of the macro-distortion tensor gives the macro-rotational vector $\varphi_i=-1/2\varepsilon_{kli}u_{k,l}$, where ε_{ijk} is the alternating tensor. It is seen that the macro-rotation vector and the distortion tensor are fully determined by the components of the displacement vector $\boldsymbol{u}(x_i)$.

   Next, assume the material point P as a centroid of a micro-volume of the originally inhomogeneous medium. This volume element defines the scale of resolution of the envisaged continuum theory. Effects below this characteristic scale are ignored. This volume element could not be constricted to the point because of the microstructure of the material. A particular choice of the micro-volume size is not important here. It suffices to mention that in general, the micro-volume size is supposed to be (a) much larger than the microstructure size to asymptotically satisfy the requirement for the micro-volume to be representative, ie contain sufficient number of elements of the microstructure and; (b) much smaller than the external size such as the dimension of the problem or a characteristic length of the load redistribution (eg, wave length), to asymptotically satisfy the requirement for the micro-volume to be infinitesimal. Furthermore its shape has to reflect the material symmetry of the material to be modelled.
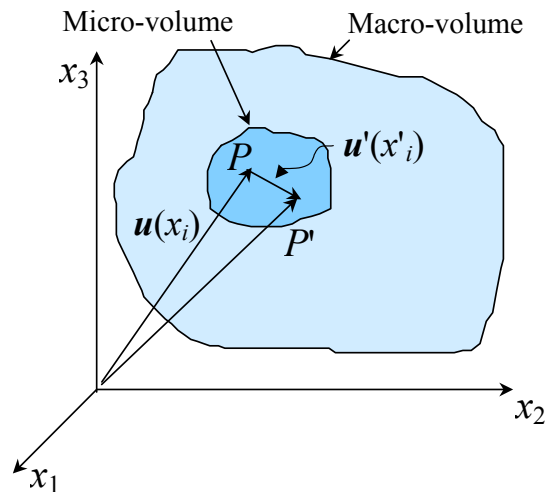

Figure 1. Macro- and micro-volumes and the relationship between the macro- and micro-displacements.

   We now introduce another local Cartesian coordinate system with the origin at P. An arbitrary point P' of the micro-volume has the micro-coordinates $x'_1x'_2x'_3$. The vector connecting P and P' will be called the micro-displacement vector and denoted as $\boldsymbol{u'}(x'_i)$. The

micro-displacement vector characterizes the displacement of the point P' within the micro-particle (micro-volume element).

The displacement of the point P' being a point of the macro-volume is given by the sum of the macro-displacement vector $\boldsymbol{u}(x_i)$ and the micro-displacement vector $\boldsymbol{u}'(x'_i)$. Expanding the components of the micro-displacement vector into the Taylor series at the vicinity of the point P one gets the correspondent coordinates of the displacement vector of the point P':

$$u_i(x) + u'_i(x') = u_i(x) + u'_i(0) + u'_{i,j}(0)x'_j + \frac{1}{2}u'_{i,jk}(0)x'_j x'_k + ..., \tag{1.1}$$

where $u'_i(0) \overset{def}{=} 0$, $x \overset{def}{=} (x_1, x_2, x_3)$, $x' \overset{def}{=} (x'_1, x'_2, x'_3)$.

The underlying assumption behind the equation (1.1) is that the displacements within the representative volume are analytic and can be represented by Taylor expansions round point P. As discussed above (conditions (a) and (b)), the size of the volume element h must be much smaller than the macro-volume characteristic dimension L and much bigger than the microstructure size a in a sense that the continuum approximation is a double asymptotics as $h/L \rightarrow 0$ and $a/h \rightarrow 0$ (eg, [4-6]). As a result of this asymptotic transition, we have a continuum that permits the usual description based on the established rules of differential geometry. The only difference from a conventional continuum is that each point may have additional DOF namely the higher order polynomial coefficients in (1.1) enabling the consideration of deviations of the deformation from the mean values within a representative volume element.

The term $u'_{i,j}$ provide us with nine micro-distortion components: three micro-rotations and six micro-strains. If for simplicity we take into account only the anti-symmetric part, we arrive at a continuum with 6 DOF (three translational DOF, the macro-displacements u_i, and three rotational ones, micro-rotations φ_i). This is the Cosserat theory or the theory of micro-polar elasticity (eg, Mindlin and Tiersten [7]; Nowacki [2]; Eringen [8]; Eringen and Kafadar [9]). The rotational degrees of freedom are very often referred to as the Cosserat rotations giving tribute to the brothers Cosserat who were the first to propose such a theory.

Further generalizations can be obtained by including the symmetric part of the microgradients into the model as well and/or by keeping the next term of the Taylor expansion $u'_{i,jk}$ bringing the total number of DOFs to 36, Mindlin [3].

It should be emphasized that the micro-deformations in the expansion (1.1) are independent in general from the macroscopic deformation gradient. The relationship between the macro-and the micro deformation is established by means of additional constitutive relationships.

The higher-order gradient theories necessitate the introduction of additional stress tensors which are conjugate to the additional deformation measures (eg, couple or moment stresses in the Cosserat type theories; double forces tensor in the Mindlin continuum, etc). In the elasticity theories, these new stress tensors can normally be obtained by differentiating the variation of an elastic potential (the elastic energy density) with respect to the variation of the deformation measures. The equations of equilibrium or motion also have to be obtained for additional stress factors in the higher-order gradient theories. It should also be mentioned that the formulation of boundary value problems maybe in terms of displacements complemented by the additional DOF's (for instance, rotations in the Cosserat theory) or in terms of the stress tensors complemented by the conjugates of the additional DOF's (for instance, couple/moment stresses in the Cosserat theory) or in a mixed form.

It is well known that the governing equations of the continuum have to be translational and rotational invariant. This requirement yields exactly 2X3 balance equations. Translational invariance requires the consideration of linear momentum; rotational invariance requires the consideration of angular momentum. The equations of motion in the standard theories result from the moment balance, while the moment of momentum balance gives the symmetry of stress tensor. In the Cosserat theories both momentum balance and moment of momentum balance are used, each contributing three equations. An interesting question for higher-order theories would be where to get the additional equations of motion/equilibrium from. At present, this question is still open[1], as no other fundamental hypotheses similar to the hypotheses of the isotropy and homogeneity of space and time have been formulated yet. That is why gradient enhanced theories become increasingly popular and used. They do not require additional motion/equilibrium equations but at the same time allow one to include the strain gradients into the formulation. This in reality does not add new DOF, but increases the order of governing partial differential equations.

Mindlin [3] used the Hamilton's principle for independent variations, which were his 12 DOF, and obtained twelve equations of motion from the variational equation of motion. However, this approach is applicable only in elastic materials. An application of the method

---

[1] A possible remedy to obtain an extra set of equilibrium/motion equations in situations when the representative volume element is made up of homogeneous but materially distinct sub-volumes is to divide the volume element into smaller ones and write down the corresponding equations of motion/equilibrium for each of them. At least

of virtual power for derivation of the balance equations of micropolar and second gradient continua was discussed in the works of Germain [10, 11] and Maugin [12].

The second approach (homogenisation by integral transformation) involves the introduction of a non-local (integral) constitutive law (when the long-range interactions between the particles need to be accounted for, eg [13]). This in general means that the stress components depend on the strains at all points of the continuum albeit with weight decreasing with distance from the point of interest. In essence, this approach shifts the procedure of homogenisation from the definition of deformation measures (by introducing the volume element) to the constitutive relationships. Both approaches can be combined leading to non-local theories with additional degrees of freedom.

Non-local homogenisation strategies of the discrete materials were introduced by Kröner [14], Kröner and Datta [15], Kunin and Waisman [16], Kunin [13, 17] and Eringen [18] for periodical microstructures. The homogenisation was performed by trigonometric interpolation of the discrete field of displacements and rotations of the particles. In those theories the particle centres are assumed to be situated at the nodes of a regular grid. This leads to non-local stress-deformation relationships reflecting the fact that the values of interpolating polynomial at a point are sensitive to the values at the other points. The kernels of the non-local relationship are expressed through the Kunin's analog of the Dirac-delta function which "remembers" the microstructure size.

Specifically, in the case of a three-DOF continuum this homogenisation procedure leads to a non-local continuum (with the same three DOF), the non-local stress-strain relationship and the non-local stresses satisfying the conventional equations of equilibrium or motion. In the following it will be demonstrated that in a continuum with six DOF, the Cosserat continuum, this homogenisation strategy leads to a non-local Cosserat continuum. Subsequently, in this continuum one comes up with the non-local constitutive equations in which stresses and moment stresses are expressed through the deformation measures (strains and curvatures). Non-local stresses and moment stresses satisfy exactly the same equations of equilibrium or motion as in the case of a "local" or "conventional" Cosserat theory. We would like to mention here that Kunin [17] also considered a quasi six-DOF continuum, in which the three

---

in this way the lever-arm (the subdivision size) can be brought into the formulation in order to get the third order double forces tensor with the balance equation for its components.

rotational DOF's are equal to the three rotations of the standard continuum. In Section 2 we represent a generalisation of Kunin's method to the case of independent rotations.

The major difference between local and non-local continua is that in the latter the stresses and couple or moment stresses become pseudo- stresses as they no longer refer to an elementary area, but to a finite volume. This obviously contradicts the Cauchy-Euler principle. The question arises why the equations of equilibrium should necessarily hold in their "conventional", local form when the interaction between the parts of the body is not of the surface nature; it is transmitted not only through the surface, but through the volume.

For the considered periodic case, a justification of the conventional form of the equations of equilibrium/motion will be offered when a non-local orthotropic Cosserat continuum model will be constructed for non-interacting identical chains of granulates. Starting from the discrete medium consisting of, for example, particles having translational and rotational DOF's, it is possible to obtain the Lagrange equation of motion. It turns out that the Lagrange equations are formally identical to the equations of a local Cosserat continuum with non-local constitutive relations. This finding supports the adoption of the "usual" local conservation laws in connection with non-local continua.

In general, the choice of the kernels is based on purely mechanistic or phenomenological considerations (eg, [19, 20]), material symmetry combined with a choice of the size of the domain of influence. Unfortunately and in particular in 3D these requirements do not constrain the possible variety of kernel forms significantly. This "inconvenience" is rather difficult to overcome, as the kernel is a function in principle of all variables of the continuum model. This poses considerable difficulties in determining possible kernel forms from experiments.

The phenomenological approach does not address the question of the validity of local conservation laws and the physical significance of Cauchy stresses in the presence of non-local constitutive laws. These issues can only be answered and follow naturally if the model equations are derived from a micro-mechanical model by means of a suitable homogenisation procedure.

Alternatively, non-local operators on strains are used in their own right as substitutes for local strains in damage loading function (de Borst *et al*. [21]) leading to non-local damage models (eg, Pijaudier-Cabot and Bazant [22]; Bazant and Pijaudier-Cabot [23]; Pijaudier-Cabot [24]).

Finally we mention a selection of developments (by no means complete), we consider relevant to the topic of this paper: macroscopic modelling of layered materials was conducted

by Mühlhaus [25], Zvolinskii and Shkhinek [26], Adhikary and Dyskin [27]. In this 2D modelling the role of the Cosserat rotation (only one rotation in this case) was played by the rotation of the neutral axis of the layer (the deflection gradient), while the moment stresses were the bending moment per unit area in the cross-sections of the layer. Mühlhaus [28] and Mühlhaus and Hornby [29, 30] modified the model of layered materials by introducing a different rotation measure, which is the relative deformation gradient. Mühlhaus [25] and Sulem and Mühlhaus [31] developed a model for a blocky material (the material broken into rectangular blocks). Cosserat type theories for random packing of granulates were also developed, for instance, by Mühlhaus and Vardoulakis [32], Mühlhaus *et al* [33], Chang and Ma [34]. A combination of a Cosserat continuum and a higher-order gradient continuum for granular materials has been derived by Mühlhaus and Oka [35] and Mühlhaus and Hornby [36].

Additional DOF's also appear in a new numerical fracture mechanics method (Wells and Sluys [37]). In this method the additional DOF's are associated with the distribution of displacement discontinuity introduced to model crack evolution.

1.2. Homogenisation methods

Homogenisation as the main method of constructing continuum descriptions of a discrete material has always been the corner stone of continuum mechanics. It was the main simplifying factor and for centuries provided a powerful means to model solid bodies as a mathematical continuum rather than a collection of elements the solids are composed of. The first and simplest approach was not to consider the scale of the microstructure at all, but to smear it, so to speak. The introduction of the concept of the representative volume element served this purpose perfectly. Many significant problems were and are formulated and solved within the framework of classical elasticity and plasticity theories. However, restrictions of smearing the microstructure were felt mainly where the microstructure was essential to model and thus could not be ignored. As a result, more sophisticated continuum theories became high in demand around the late 1980's and so were adequate homogenisation strategies. The following is a sampling of the most important homogenisation procedures:

1. *Averaging over volume element adopted in the theory of effective characteristics* (eg, Hill [38]; Mori and Tanaka [39]; Christensen [40]; Hashin [41]; Kachanov [42]; Nemat-Nasser and Horii [43]; Germanovich and Dyskin [5]; Krajcinovic [44]; Cambou [45]).

Homogenisation produces a set of macroscopic elastic moduli based on the properties of the microstructure. These micro-structural constants are called effective characteristics, from which the name of the method derives.

2. *Homogenisation method applied to materials with randomly varying elastic properties* based on averaging over realizations (ensemble averaging), (Savin and Khoroshun [46]; Khoroshun [47]).

3. *A group of methods based on modelling of periodically regular microstructure* such as periodical system of defects/inclusions, layers, regular granular packing (eg, Duffy and Mindlin [48]; Deresiewicz [49]; Meguid and Kalamkarov [50]). This group of methods exploits the fact that the microstructure is positioned in periodical cells and the problem is solved for a representative defect. Then by using the periodicity, the solution for the whole domain is sought by looking for suitable periodic functions accompanied by corresponding periodic boundary conditions at the cell boundaries (eg, Vanin [51]; Nemat-Nasser and Horii [43]; Cambou [45]).

4. *Homogenisation by integral transformations* (Kunin [13, 17]). This is a special method of homogenisation applied to periodical structures only. The method is based on the trigonometrical interpolation. The discrete medium is replaced with a continuous one such that the continuous values of field variables coincide with the discrete ones at the nodes and give some values in between by using the above trigonometrical interpolation.

5. *Homogenisation by differential expansions* (eg, Mühlhaus and Oka [35]; Maugin [52]; Suiker *et al* [53, 54, 55]). The method is based on expanding the field variables into the Taylor series once a strategy to relate the discrete variables to continuum variables is established. This method allows for higher-order theories derivations if a way to identify correspondent derivatives of the field variables in the Taylor expansions as higher-order terms can be found.

1.3. Continuum modelling of granular materials

Depending on the packing density, granular materials can behave like solids or like fluids. If the packing is dense, granular material behaves solid-like. Large (finite) deformations are not ruled out. For loose packings, granular material may behave fluid-like. Here we concentrate on the first type. For a discussion of the fluid-like regime see eg, Mühlhaus and Hornby [36]. We concentrate on elastic models for simplicity since the emphasis is on the homogenisation procedure and not on constitutive details.

Discrete and continuum models represent two main streams of modelling of mechanical behaviour of granular materials. In the former approach granular materials are modelled as a discrete system using, for example, the discrete element method. Many models are developed in the framework of this approach (eg, Satake [56]; Tüzün and Heyes [57]; Thornton [58]; Mühlhaus *et al* [59]). Equations of motion are solved for each particle in the assembly: the particle is subjected to momentum or even mass transfer from neighbouring particles. The number of equations to solve is naturally quite large requiring powerful computers. On top of that, direct computer simulations would require detailed information (geometrical and mechanical) of all grains in the assembly. This kind of information is usually hard to obtain or not available. In other words, the computational accuracy achievable in principle by this method much exceeds the accuracy of the input data available – hardly an efficient way of modelling.

In the continuum approach the equations of motion are derived for a volume element, governing equations describing constitutive behaviour are formulated by using the continuum stress-strain concepts. Continuum models can be classified as phenomenological and microstructural. Phenomenological modelling (eg, Gudehus [60]) is based on postulating the constitutive equations, which necessitates a considerable amount of testing and model calibration.

Microstructural continuum modelling was extensively developed over the past few years as an alternative or a strategy to provide constrains for phenomenological constitutive models. The benefit of the microstructural approach is that it results into rational estimates of the model parameters.

For applications of microstructural approach see the papers by Duffy and Mindlin [48], Deresiewicz [49], Digby [61], Walton [62], Bathurst and Rothenberg [63], Chang [64], Jenkins [65], Mühlhaus and Oka [35]. The principles of microstructural modelling have been revisited recently by Suiker *et al* [53, 54, 55], Cambou *et al* [66].

The first simple micro-polar (Cosserat) type theories for random packing granulates were developed by Mühlhaus and Vardoulakis [32], Mühlhaus *et al* [33], Chang and Ma [34]. Both stresses and moment stresses were introduced, but the contact particle interaction was less sophisticated than in the more recently developed theories (Fleck and Cocks, eds., [67]). For example, moment stresses were attributed to the tangential component of the contact force and only resistance to the relative particle displacements was introduced into the contact relations (eg, Mühlhaus *et al* [33]).

Further development of pure Cosserat type theories for randomly packed assemblies went in the direction of more sophisticated and refined particle interaction modelling. This includes both contact force and moment exerted onto a reference particle, as well as the resistance of the particles to both their relative displacements and relative rotations at the contact points. These refinements were implemented by Pasternak and Mühlhaus [68, 69, 70]. Orthotropic Cosserat and non-local Cosserat continuum models for non-interacting chains of granulates were developed by Mühlhaus *et al* [6], Pasternak and Mühlhaus [71, 72], see details in Section 2.

The wide variety of approaches discussed above suggests that a comparative study of the different methodologies may be useful in order to assess the quality of the approximation of the different homogenisation methods.

For simplicity we consider a model example of microstructure: 1D non-interacting chains. The structural bonds determine the material behaviour only in one direction. This case of non-interacting chains of spheres is artificial and cannot be seriously thought as an example of granular material. It is selected to serve a special purpose – to have a structure for which the exact solution would not be very difficult to find and to provide a testing ground for comparison of homogenisation methods. We will then proceed to investigation of wave propagation in granular materials with internal rotational degrees of freedom.

2. HOMOGENISATION OF 1D STRUCTURES

In the following we demonstrate how additional rotational degrees of freedom arise naturally by mathematical homogenisation of a discrete system. For this purpose, a simple periodic discrete model of spheres connected to each other by both rotational and translational springs will be considered. This model allows the analytical derivation of a general closed form solution.

The aim of this section is to investigate two homogenisation techniques. One of them produces an anisotropic Cosserat continuum and the other one produces a non-local Cosserat continuum. A boundary value problem of a vertical duct will be considered in order to establish how accurately the Cosserat and non-local models describe the behaviour of the granular materials.

2.1. Model formulation

In many cases, generalised continuum theories provide a convenient framework for the approximate representation of an originally discrete model. In order to analyse different homogenisation techniques we consider a simple material consisting of one dimensional, parallel chains of identical, spherical grains. We suppose that the chains do not interact with each other. The grains in a chain are connected by translational shear springs of stiffness k and rotational springs of stiffness k_φ (Figure 2), r is the sphere radius. The grains in neighbouring chains are not connected and move independently.
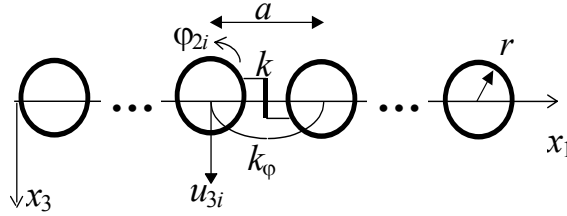

Figure 2. 1D chain of spherical grains connected by translational (shear) and rotational springs.

The potential (elastic) energy of a single chain in the system reads

$$U_1 = \frac{1}{2}k\sum_i \left((u_i - u_{i-1}) + (a/2)(\varphi_i + \varphi_{i-1})\right)^2 + \frac{1}{2}k_\varphi \sum_i (\varphi_i - \varphi_{i-1})^2 \qquad (2.1)$$

with the potential energy density referred to the *i*-th sphere being:

$$W_i = \left(2\eta a^3\right)^{-1}\left\{k\left((u_{3i} - u_{3i-1}) + (a/2)(\varphi_{2i} + \varphi_{2i-1})\right)^2 + k_\varphi(\varphi_{2i} - \varphi_{2i-1})^2\right\}. \qquad (2.2)$$

Here a designates the spacing of the mass centres of neighbouring spheres, and $a^{-2}\eta^{-1}$ is the number of chains per unit area of cross-section.

We note here that the rotational springs are important in this arrangement, since neglecting the resistance to rotation ($k_\varphi \to 0$) makes the energy lose its positive definiteness.

The equations of motion for the spheres are:

$$m\ddot{u}_{3i} - k(u_{3i+1} - 2u_{3i} + u_{3i-1}) - k(a/2)(\varphi_{2i+1} - \varphi_{2i-1}) = q_{3i}, \qquad (2.3_1)$$

$$J\ddot{\varphi}_{2i} + k(a/2)(u_{3i+1} - u_{3i-1}) + k(a^2/4)(\varphi_{2i+1} + 2\varphi_{2i} + \varphi_{2i-1}) - k_\varphi(\varphi_{2i+1} - 2\varphi_{2i} + \varphi_{2i-1}) = M_{2i} \quad (2.3_2)$$

where u_{3i}, φ_{2i} are the independent Lagrange coordinates, q_{3i} and M_{2i} are applied load and moment at *i*-th sphere respectively, $J=2mr^2/5$ is the moment of inertia of the sphere.

2.2. Homogenisation by differential expansion (Cosserat continuum)

We replace the finite difference expressions in (2.2) with corresponding differential expressions. Truncation of the Taylor expansions in *a* after the second order terms gives the following approximation

$$W(x_1) = \left(2\eta a^3\right)^{-1}\left\{ k\left(\frac{\partial u_3}{\partial x_1}\right)^2 a^2 + 2ka\frac{\partial u_3}{\partial x_1}\varphi_2 a + ka^2\varphi_2^{\,2} + k_\varphi\left(\frac{\partial \varphi_2}{\partial x_1}\right)^2 a^2\right\}. \tag{2.4}$$

Differentiation of the energy density with respect to the Cosserat deformation measures, viz. strains and curvatures,

$$\gamma_{13} = \frac{\partial u_3}{\partial x_1} + \varphi_2, \ \kappa_{12} = \frac{\partial \varphi_2}{\partial x_1}, \tag{2.5}$$

gives

$$\sigma_{13} = k(\eta a)^{-1}\gamma_{13}, \ \mu_{12} = k_\varphi(\eta a)^{-1}\kappa_{12}. \tag{2.6}$$

Introduction of body force f_3 and moment m_2 and consideration of momentum and angular momentum equilibrium yield

$$\frac{\partial \sigma_{13}}{\partial x_1} + \rho f_3 = \rho\ddot{u}_3, \ \frac{\partial \mu_{12}}{\partial x_1} - \sigma_{13} + \rho m_2 = \tilde{J}\ddot{\varphi}_2, \tag{2.7}$$

where $\rho = \dfrac{m}{a^3\eta}$ is the density, $\tilde{J} = \dfrac{J}{a^3\eta}$ is rotational inertia per unit volume or density of rotational inertia.

Equations (2.5)-(2.7) formally represent a 1D Cosserat continuum (eg, [2]). Every point of this continuum has two degrees of freedom: u_3 represents the displacement, while φ_2 is being identified as the independent rotational degree of freedom, the Cosserat rotation. Mechanically speaking, the obtained continuum equations describe a 3D orthotropic Cosserat continuum (all other components of stress and moment stress tensors and corresponding deformation measures are zero). Formally, after suitable reinterpretation of the model

parameters[2] one obtains the governing equations of a Timoshenko beam (eg, [28, 73]). In this case φ_2 represents the rotation of the beam cross-section and u_3 is the displacement of its neutral fibre.

After substituting constitutive equations (2.6) into equations of motion (2.7) we obtain the Cosserat equations of motion (the Cosserat equivalent of Lamé equations):

$$\frac{k}{\eta a}\left(\frac{\partial^2 u_3}{\partial x_1^{\,2}} + \frac{\partial \varphi_2}{\partial x_1}\right) + \rho f_3 = \rho \ddot{u}_3, \tag{2.8$_1$}$$

$$\frac{1}{\eta a}\left(k_\varphi \frac{\partial^2 \varphi_2}{\partial x_1^{\,2}} - k\frac{\partial u_3}{\partial x_1} - k\varphi_2\right) + \rho m_2 = \frac{J}{a^3 \eta}\ddot{\varphi}_2. \tag{2.8$_2$}$$

Next we homogenise discrete equations of motion (2.3$_1$)-(2.3$_2$) and compare the result with the obtained Cosserat equations of motion (2.8$_1$)-(2.8$_2$). For the derivation of the continuum version of equations (2.3$_1$)-(2.3$_2$) we first replace the discrete coordinate by a continuous coordinate, ie $ai \rightarrow x$ as outlined for example by Mühlhaus and Oka [35] $u_{3i} \mapsto u_3(x_1)$, $u_{3i} \mapsto u_3(x_1)$, $\ddot{u}_{3i} \mapsto \ddot{u}_3(x_1)$, $\varphi_{2i} \mapsto \varphi_2(x_1)$, $\ddot{\varphi}_{2i} \mapsto \ddot{\varphi}_2(x_1)$, $q_{3i} \mapsto q_3(x_1)$, $M_{2i} \mapsto M_2(x_1)$, $u_{3i\pm1} \mapsto u_3(x_1 \pm a)$, $u_{3i\pm1} \mapsto u_3(x_1 \pm a)$, $\varphi_{3i\pm1} \mapsto \varphi_3(x_1 \pm a)$.

The equations (2.3$_1$)-(2.3$_2$) can formally be written in a homogenised (continuous) form by introducing continuous functions $u_3(x)$, $\varphi_2(x)$ which coincide with u_{3i} and $\varphi_{2i}(x)$ at discrete points $x = ai$ and assume some values in between:

$$m\ddot{u}_3(x_1) - k[u_3(x_1 + a) - 2u_3(x_1) + u_3(x_1 - a)] - k(a/2)[\varphi_2(x_1 + a) - \varphi_2(x_1 - a)] = q_3(x_1) \tag{2.9$_1$}$$

$$J\ddot{\varphi}_2(x_1) + k(a/2)[u_3(x_1 + a) - u_3(x_1 - a)] + k(a^2/4)[\varphi_2(x_1 + a) + 2\varphi_2(x_1) + \varphi_2(x_1 - a)] -$$

$$- k_\varphi[\varphi_2(x_1 + a) - 2\varphi_2(x_1) + \varphi_2(x_1 - a)] = M_2(x_1). \tag{2.9$_2$}$$

These formal equations will form the starting point for the homogenisation below.

Following Mühlhaus and Oka [35], the equations (2.9$_1$)-(2.9$_2$) can be homogenised by replacing the finite differences with the Taylor series expansions, keeping terms of the second order in a and normalising the obtained equations by the volume (i.e. dividing by $a^3\eta$) one eventually has

---

[2] k_φ/a is interpreted as the bending stiffness, k/a as the shear modulus.

$$\frac{k}{\eta a}[u_3''(x_1) + \varphi_2'(x_1)] + O(1) + \frac{q_3(x_1)}{a^3 \eta} = \rho \ddot{u}_3(x_1), \tag{2.10$_1$}$$

$$\frac{1}{\eta a}\Big[k_\varphi \varphi_2''(x_1) - ku_3'(x_1) - k\varphi_2(x_1)\Big] + O(1) + \frac{M_2(x_1)}{a^3 \eta} = \frac{J}{a^3 \eta}\ddot{\varphi}_2(x_1), \tag{2.10$_2$}$$

where $\rho = m/(a^3\eta)$.

Comparison of (2.8$_1$)-(2.8$_2$) with (2.10$_1$)-(2.10$_2$) leads to the conclusion that the equations of motion in the Cosserat approximation (2.8$_1$)-(2.8$_2$) give the same leading terms as the approximation of the discrete (exact) equations of motion (2.3$_1$)-(2.3$_2$). Hence, the Cosserat theory gives exact terms up to the first order in *a* inclusive. One could anticipate that the terms of order higher than *a* would be captured by higher order theories. The resolution of the theory is *a*, ie all the "events" smaller than *a* are not seen (recognised) by the Cosserat continuum, which is natural since the *a* is a length scale or microstructural parameter of this Cosserat theory.

This Cosserat theory has also another length scale parameter. The second parameter is given by the square root of the ratio of the stiffness of the rotational spring k_φ to the translational spring stiffness *k* and has the dimension of length.

Note that the limit $a\rightarrow0$ in both (2.8$_1$)-(2.8$_2$) and (2.10$_1$)-(2.10$_2$) should be understood as $a/L\rightarrow0$, where *L* is the size of redistribution of the load (ie an external size). In other words, in the above calculations the normalisation in which *L*=1 is presumed.

It follows from the above analysis that the Cosserat equations of motion through displacements and rotations (a kind of "Lamé equations" for the Cosserat continuum) can be obtained either by the direct homegenisation of the discrete equations of motion or by homogenisation by differential expansions of the potential energy density of the discrete system provided that the same order of approximation is maintained in both cases.

The outlined strategy of homogenisation by differential expansions allows one to formulate the appropriate continuum description of the discrete system. The homogenised potential energy density of the mechanical system has the meaning of the elastic energy density in the continuum sense with subsequent introduction of the deformation measures. Once the constitutive equations have been recovered, the Cosserat "Lamé equations" are obtained in a usual fashion by substituting the governing equations into the motion equation. Thus, the boundary value problem can be formulated accompanied by boundary conditions. This approach can be virtually adjusted to any microstructural particles arrangements.

2.3. Homogenisation by integral transformation (non-local Cosserat continuum)

Here we consider another homogenisation strategy – homogenisation by integral transformations. Kunin's [13] homogenisation procedure for discrete periodical structures is based on the trigonometrical interpolation of discrete functions. For the material consisting of independent periodical chains of grains we have:

$$\begin{pmatrix} u_3(x_1) \\ \varphi_2(x_1) \end{pmatrix} = a \sum_i \begin{pmatrix} u_{3i} \\ \varphi_{2i} \end{pmatrix} \delta_K(x_1 - ia), \quad \begin{pmatrix} u_{3i} \\ \varphi_{2i} \end{pmatrix} = \int \delta_K(x_1 - ia) \begin{pmatrix} u_3(x_1) \\ \varphi_2(x_1) \end{pmatrix} dx_1, \quad \delta_K(x) = (\pi x)^{-1} \sin \frac{\pi x}{a}. \quad (2.11)$$

The application of (2.11_1) to the discrete equations of motion (2.3) yields the non-local equations of motion (non-local Lamé equations):

$$k \int_{-\infty}^{+\infty} [2\delta_K(x_1 - y_1) - \delta_K(x_1 - y_1 - a) - \delta_K(x_1 - y_1 + a)] u_3(y_1) dy_1 +$$

$$+ k(a/2) \int_{-\infty}^{+\infty} [\delta_K(x_1 - y_1 - a) - \delta_K(x_1 - y_1 + a)] \varphi_2(y_1) dy_1 = q_3(x_1) - m\ddot{u}_3(x_1), \quad (2.12_1)$$

$$k(a/2) \int_{-\infty}^{+\infty} [\delta_K(x_1 - y_1 + a) - \delta_K(x_1 - y_1 - a)] u_3(y_1) dy_1 +$$

$$+ k(a^2/4) \int_{-\infty}^{+\infty} [\delta_K(x_1 - y_1 + a) + 2\delta_K(x_1 - y_1) + \delta_K(x_1 - y_1 - a)] \varphi_2(y_1) dy_1 + \quad (2.12_2)$$

$$+ k_\varphi \int_{-\infty}^{+\infty} [2\delta_K(x_1 - y_1) - \delta_K(x_1 - y_1 + a) - \delta_K(x_1 - y_1 - a)] \varphi_2(y_1) dy_1 = M_2(x_1) - J\ddot{\varphi}_2(x_1).$$

These equations are essentially a representation of (2.9).

In order to obtain the constitutive relationship we consider the potential energy of a chain (2.1) since a structure we are studying is essentially one-dimensional. Inserting (2.11_1) into (2.1), integrating the result by parts and assuming that functions u and φ and their derivatives decay strongly enough at infinity to make the non-integral terms zero, leads to the following representation of the elastic energy of the chain:

$$U_1 = \frac{k}{2a}\iint[2C(x_1-y_1)-C(x_1-y_1-a)-C(x_1-y_1+a)]\gamma_{13}(x_1)\gamma_{13}(y_1)dx_1dy_1 +$$

$$+\frac{k}{a}\iint[2K(x_1-y_1)-K(x_1-y_1-a)-K(x_1-y_1+a)]\kappa_{12}(x_1)\gamma_{13}(y_1)dx_1dy_1 +$$

$$+\frac{k}{2a}\iint[2K_1(x_1-y_1)-K_1(x_1-y_1-a)-K_1(x_1-y_1+a)]\kappa_{12}(x_1)\kappa_{12}(y_1)dx_1dy_1 +$$

$$+\frac{k}{2}\iint[C(x_1-y_1-a)-C(x_1-y_1+a)]\gamma_{13}(x_1)\kappa_{12}(y_1)dx_1dy_1 + \qquad (2.13)$$

$$+\frac{k}{2}\iint[K(x_1-y_1-a)-K(x_1-y_1+a)]\kappa_{12}(x_1)\kappa_{12}(y_1)dx_1dy_1$$

$$+\frac{ka}{8}\iint[2C(x_1-y_1)+C(x_1-y_1-a)+C(x_1-y_1+a)]\kappa_{12}(x_1)\kappa_{12}(y_1)dx_1dy_1 +$$

$$+\frac{k_\varphi}{2a}\iint[2C(x_1-y_1)-C(x_1-y_1-a)-C(x_1-y_1+a)]\kappa_{12}(x_1)\kappa_{12}(y_1)dx_1dy_1$$

where $C''(x) = -\delta_K(x)$, $K'(x) = C(x)$, $K_1^{''}(x) = -C(x)$ and the introduced Cosserat deformation measures have the form

$$\gamma_{13} = \frac{\partial u_3}{\partial x_1} + \varphi_2, \quad \kappa_{12} = \frac{\partial \varphi_2}{\partial x_1}. \qquad (2.14)$$

The choice of deformation measures (2.14) was dictated by the wish to be consistent with the previous section as the intention to build a non-local Cosserat continuum was envisaged. In fact, this is the only possible way to introduce the deformation measures that would be invariant with respect to the rigid body translation and rotation. Indeed, for the rigid body translation u_3=const, φ_2=0, γ_{13}=0, κ_{12}=0; similarly for the rigid body rotation

u_3= -$x_1\varphi_2$, φ_2=const, γ_{13}=$\partial u_3/\partial x_1$+ φ_2= -φ_2+φ_2=0, κ_{12}=0.

Consider the energy of the whole body $U=N_1N_2U_1$, where N_1, N_2 are numbers of chains in the directions x_2 and x_3 respectively. Variation of the energy is

$$\delta U = \int_V \delta W(x_1,x_2,x_3)dv = \eta a^2 N_1 N_2 \int_{-\infty}^{+\infty}\delta W(x_1)dx_1 = \eta a^2 N_1 N_2 \int_{-\infty}^{+\infty}(\sigma\delta\varepsilon + \mu\delta\kappa)dx_1, \qquad (2.15)$$

where $W(x_1,x_2,x_3)$ is the specific potential energy at point $x=(x_1,x_2,x_3)$, $\eta^{1/2}a$ is the spacing between non-interacting chains of the spatial assembly. Since $\delta U=N_1N_2\delta U_1$ the variation of $U_1=U_1(\gamma_{13}, \kappa_{12})$ in (2.13) with subsequent extraction of δW in (2.15) and the introduction of the stress and moment stress

$$\sigma_{13}(x) = \frac{\delta W}{\delta\gamma_{13}(x)}, \quad \mu_{12}(x) = \frac{\delta W}{\delta\kappa_{12}(x)} \qquad (2.16)$$

yield the following expressions for the stress and the moment stress:

$$\sigma_{13}(x_1) = \left(\sqrt{\eta}a\right)^{-2} \{E \int_{-\infty}^{+\infty} [2C(x_1 - y_1) - C(x_1 - y_1 - a) - C(x_1 - y_1 + a)]\gamma_{13}(y_1)dy_1 -$$

$$- E \int_{-\infty}^{+\infty} [2K(x_1 - y_1) - K(x_1 - y_1 - a) - K(x_1 - y_1 + a)]\kappa_{12}(y_1)dy_1 + \qquad (2.17)$$

$$+ E(a/2) \int_{-\infty}^{+\infty} [C(x_1 - y_1 - a) - C(x_1 - y_1 + a)]\kappa_{12}(y_1)dy_1\}, \quad E = k/a,$$

$$\mu_{12}(x_1) = \left(\sqrt{\eta}a\right)^{-2} \{E(a/2) \int_{-\infty}^{+\infty} [C(x_1 - y_1 + a) - C(x_1 - y_1 - a)]\gamma_{13}(y_1)dy_1 +$$

$$+ E(a^2/4) \int_{-\infty}^{+\infty} [2C(x_1 - y_1) + C(x_1 - y_1 - a) + C(x_1 - y_1 + a)]\Omega_{12}(y_1)dy_1 +$$

$$+ E_\varphi \int_{-\infty}^{+\infty} [2C(x_1 - y_1) - C(x_1 - y_1 - a) - C(x_1 - y_1 + a)]\Omega_{12}(y_1)dy_1 +$$

$$+ E \int_{-\infty}^{+\infty} [2K(x_1 - y_1) - K(x_1 - y_1 + a) - K(x_1 - y_1 - a)]\gamma_{13}(y_1)dy_1 + \qquad (2.18)$$

$$+ E \int_{-\infty}^{+\infty} [2K_1(x_1 - y_1) - K_1(x_1 - y_1 + a) - K_1(x_1 - y_1 - a)]\Omega_{12}(y_1)dy_1 +$$

$$+ Ea \int_{-\infty}^{+\infty} [K(x_1 - y_1 - a) - K(x_1 - y_1 + a)]\Omega_{12}(y_1)dy_1\}, \quad E_\varphi = k_\varphi/a.$$

It is seen that the homogenisation by integral transformations produces non-local constitutive relationships with oscillating kernels. The origin of this particular type of non-locality is in the fact that the interpolation function for a given set of u_{3i}, φ_{2i} is unique, and hence the alteration of any local value leads to the change of the whole function.

Integrating the non-local "Lamé equations" (2.12) by parts, extracting the expressions (2.17), (2.18) and accounting for volume forces and moments yields the following Euler-Lagrange equations:

$$\frac{d\sigma_{13}(x_1)}{dx_1} + \frac{q_3(x_1)}{a^3\eta} = \frac{m}{a^3\eta}\ddot{u}_3(x_1), \quad \frac{d\mu_{12}(x_1)}{dx_1} - \sigma_{13}(x_1) + \frac{M_2(x_1)}{a^3\eta} = \frac{J}{a^3\eta}\ddot{\varphi}_2(x_1). \qquad (2.19)$$

The form of the angular momentum balance (2.19$_2$) is standard and consistent with its Cosserat counterpart (cf. (2.7$_2$)). Stresses σ_{13}, μ_{12} are interpreted conventionally. However the constitutive relationships are non-local ie determined by the deformations of all parts of a chain. There could be another view on the non-local stresses and moment stresses. Since they are no longer referred to the elementary area they are supposed to act onto in the conventional Cauchy sense, the continuum obtained may be regarded as a pseudo- one. Nevertheless, we give the preference to the term 'non-local Cosserat continuum'.

In essence, the equations (2.14), (2.17), (2.18) and (2.19) constitute mathematically a 1D non-local Cosserat continuum. Every point of this continuum has two degrees of freedom, the displacement u_3 and the Cosserat rotation φ_2. Mechanically speaking, the obtained continuum equations describe a 3D non-local orthotropic Cosserat continuum (all other components of stress and moment stress tensors and corresponding deformation measures are zero).

Obviously, the non-local "Lamé equations" (2.12_1)-(2.12_2) can be recovered if one substitutes the non-local constitutive relationships (2.17), (2.18) into the equations of motion (2.19). This gives a displacement-rotation formulation.

2.4. Invertibility of kernels in non-local constitutive equations

Here we will discuss the issue of invertibility of the kernels in non-local constitutive equations (2.17), (2.18). One can expect that they have an inverse since their generating function, the Kunin-delta, has the inverse in contrast to the non-inversible bell-shaped Gaussian kernels often used nowadays (eg, [20]).

The discrete system with $6N$ degrees of freedom, N being the number of the particles in it, is defined by the $6N$ Lagrange coordinates, displacements and rotations, u_i, φ_i. If the forces and moments q_i, M_i are applied to the mechanical system the one-to-one correspondence between the loads applied to the mechanical system and displacements and rotations is established by the discrete (Lagrange) equations of motion (2.3). Let A be this one-to one mapping:

$$A\begin{bmatrix} \vec{u} \\ \vec{\varphi} \end{bmatrix} = \begin{bmatrix} \vec{q} \\ \vec{M} \end{bmatrix}. \tag{2.20}$$

If the system of the discrete equations of motion can be solved for displacements and rotations of the particles, then it is given by the inverse mapping A^{-1}.

The application of the homogenisation by integral transformations (Kunin's homogenisation) (2.11) gives the homogenised continuum variables $u(x)$, $\varphi(x)$, $q(x)$, $M(x)$, governed by the homogenised equations of motion (2.3) or formally (2.20), for example in the form (2.9) or (2.12). The spaces of the discrete and continuum representations are isomorphic, Kunin [14]. Let H_1 be this isomorphism, ie H_1 establishes the isomorphism between the discrete Lagrange coordinates and their continuum counterparts, between the discrete and non-local equations of motion. Following a procedure similar to the outlined in the previous

section, non-local constitutive relationship can be obtained (eg, (2.17), (2.18)). We formally write it down as follows

$$\begin{bmatrix} \sigma_{13} \\ \mu_{12} \end{bmatrix} = K \begin{bmatrix} \gamma_{13} \\ \kappa_{12} \end{bmatrix},$$

(2.21)

where K is non-local operator acting on the strains and curvatures and producing non-local stresses and moment stresses.

The space of the discrete loads applied to the system is isomorphic to the space of the non-local stresses and moment stresses, and this isomorphism H_2 is established by the equations of equilibrium (2.19) modulo the two free constants determined by the boundary conditions. This is illustrated by the diagram on Figure 3. Thus we conclude that if $\exists A^{-1}$ then $\exists\ K^{-1}$ i.e. K is invertible. This means that kernels in non-local constitutive equations have their inverses if the initial discrete mechanical system is solvable for displacements and rotations under prescribed loads.

It is worth noting that since H_1 establishes the isomorphism between the discrete Lagrange coordinates and their continuum counterparts, ie between the discrete and non-local equations of motion, the homogenised equations (2.3) or (2.12) are exact. This means that the solution of a boundary value problem under this non-local formulation must be exact or in other words must coincide with the discrete one.

Figure 3. Isomorphism of spaces.

2.5. Random kernels

As we established above in the non-local relationships (2.17), (2.18) some of the kernels exhibit the oscillating behaviour. An interesting question is now whether the oscillating behaviour of the kernels in the non-local relationships (2.17), (2.18) will disappear if some form of randomness is introduced into the mechanical system. In other words, can the

randomness help to cure the oscillating nature of the kernels in the non-local constitutive equations, ie can we get a nice bell shape form of the kernels in this case, as presumed eg by Eringen [20]. We try to find what non-local kernels look like for the irregular arrangements of the balls in chains. Since all the kernels were generated by the Kunin-delta, it would suffice to consider a less sophisticated model in which the nature of the problem is preserved, but the number of kernels would reduce significantly.

In view of this, we consider a simple material consisting of one dimensional, parallel, non-interacting chains of identical, spherical grains as before, but now the grains in a chain are connected by translational normal springs of stiffness k_i only, r is the sphere radius, a is the interball distance as before (Figure 4). To be able to apply the homogenisation by integral transformation the inter-ball spacing is presumed constant. We assume that stiffnesses k_i are independent random variables, normally distributed with the mathematical expectations $E(k_i)=k$ and the variance $Var(k_i)=s^2$. This way the irregularity of the system is achieved. It will be enough to consider only one chain as our aim is restricted to investigating the form of the kernel rather than building a proper continuum for this model.

The potential (elastic) energy of a single chain in the system reads

$$U_1 = \frac{1}{2}\sum_i k_i (u_i - u_{i-1})^2 .$$

(2.22)

Insertion of (2.11$_1$) into (2.22) yields the following homogenisation for the potential energy:

$$U_1 = \frac{1}{2}\iint \hat{\Phi}(x,y)[u(x)-u(x-a)][u(y)-u(y-a)]dxdy,$$

(2.23)

$$\hat{\Phi}(x,y) = \sum_i k_i \delta_K (x-ia)\delta_K (y-ia) .$$
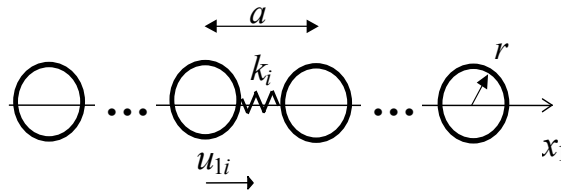
(2.24)

Figure 4. 1D chain of spherical grains connected by translational (normal) springs.

In series (2.24) k_i are independent normal variables and $\sum_i [\delta_K(x-ia)\delta_K(y-ia)]^2 < \infty$.

Therefore, for fixed (x,y) $\hat{\Phi}(x,y)$ is a normal variable (eg, [74]). Accordingly, the kernel $\hat{\Phi}$ is a normally distributed random function. Since the number of the spheres in the chain is large, the finite sums can be replaced with series, then the mathematical expectation and the variance are

$$\mathrm{E}\hat{\Phi}(x,y) = \sum_i \delta_K(x-ia)\delta_K(y-ia)\mathrm{E}k_i = \frac{k}{a}\delta_K(x-y), \tag{2.25}$$

$$Var\hat{\Phi}(x,y) = \frac{s^2\pi^{-2}}{(x-y)^2}\left\{-2(a^{-1}\delta_K(x-y)-a^{-2})\sin\frac{\pi x}{a}\sin\frac{\pi y}{a}+a^{-2}\left(\sin\frac{\pi x}{a}-\sin\frac{\pi y}{a}\right)^2\right\}. \tag{2.26}$$

The mathematical expectation is the kernel that one would obtain conducting stochastic experiment and according to (2.25) is given by Kunin-delta function (with a factor) that is oscillating. This means that the imposed randomness modelling irregularity of the particles arrangement does not remove the oscillating nature of the kernel, ie after averaging the kernel determined by the random function (2.25) does not have the Gaussian, bell-shaped form.

The variance (2.26) behaves asymptotically as $s^2a^{-4}[(\sin^2(\pi x/a))/3+1]$ at $(x-y)\to 0$ and thus does not have singularities when $(x-y)\to 0$, which is sound since the series in (2.24) is convergent.

The normally distributed function $\hat{\Phi}(x,y)$ is fully determined by its mathematical expectation, the variance and the two-point correlation function. The correlation function between any two points $\hat{\Phi}_1 \equiv \hat{\Phi}(x_1,y_1) = \sum_i k_i\delta_K(x_1-ia)\delta_K(y_1-ia)$ and

$\hat{\Phi}_2 \equiv \hat{\Phi}(x_2,y_2) = \sum_i k_i\delta_K(x_2-ia)\delta_K(y_2-ia)$ can be found as follows:

$$COV(\hat{\Phi}_1,\hat{\Phi}_2) = -s^2\pi^{-3}a^{-1}\sin\frac{\pi x_1}{a}\sin\frac{\pi y_1}{a}\sin\frac{\pi x_2}{a}\sin\frac{\pi y_2}{a}\left\{\frac{\cot\dfrac{\pi x_1}{a}}{(x_1-x_2)(x_1-y_1)(x_1-y_2)}+\right.$$

$$\left.+\frac{\cot\dfrac{\pi x_2}{a}}{(x_2-x_1)(x_2-y_1)(x_2-y_2)}+\frac{\cot\dfrac{\pi y_1}{a}}{(y_1-x_1)(y_1-x_2)(y_1-y_2)}+\frac{\cot\dfrac{\pi y_2}{a}}{(y_2-x_1)(y_2-x_2)(y_2-y_1)}\right\}. \tag{2.27}$$

It can be shown that formal limiting transition $x_1 \to x_2$, $y_1 \to y_2$ leads to $COV(\hat{\Phi}, \hat{\Phi}) = Var\hat{\Phi}$. Indeed, by taking the limit of $(x_1, y_1) \to (x_2, y_2)$ in the last formula, one arrives to the formula for the variance (2.26). This serves as an indirect verification of (2.27).

2.6. A boundary value problem. Vertical duct

Let us consider an infinitely long duct occupying the area $0 < x_1 < L$, $|x_3| < \infty$. The duct is filled with granular material modelled by identical regular chains of balls connected by translational and rotational springs (Figure 5). The boundaries of each chain are subjected to pure clamping which corresponds to the following boundary conditions: $u_3 = 0$, $\varphi_2 = 0$. The volume force of ρg is applied to every ball. Let us assume that all fields depend on x_1 only. The inertia terms $\ddot{u}_3$, $\ddot{\varphi}_2$ are neglected.

For the sake of simplicity x will be written instead of x_1, u instead of u_3, φ instead of φ_2.
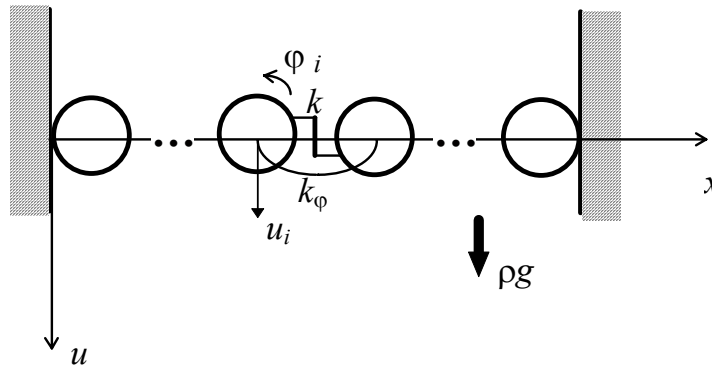

Figure 5. Model of the duct with grains.

2.6.1. Exact solution of the discrete equations of equilibrium for the duct

We now find the exact solution – the solution of the finite difference equations system (2.3) for the static case, $q_i = q$, $(q = -B\eta a^3)$, $M_i = 0$ under the following boundary conditions:

$$u_{j=0} = u_0, \; u_{j=N} = u_N, \; \varphi_{j=0} = \varphi_0, \; \varphi_{j=N} = \varphi_N. \tag{2.28}$$

The general solution of the correspondent homogeneous system:

$$-k(u_{i+1} - 2u_i + u_{i-1}) - k(a/2)(\varphi_{i+1} - \varphi_{i-1}) = 0, \quad (i = 1, ..., N-1). \tag{2.29_1}$$

$$k(a/2)(u_{i+1} - u_{i-1}) + k(a^2/4)(\varphi_{i+1} + 2\varphi_i + \varphi_{i-1}) - k_\varphi(\varphi_{i+1} - 2\varphi_i + \varphi_{i-1}) = 0 \tag{2.29_2}$$

is sought in the form $u_i = C\chi^i$, $\varphi_i = \overline{C}\chi^i$. By substituting it into (2.29) the multiple root of fourth order, $\chi = 1$, of the characteristic equation can be found. Then using the boundary conditions at j=0, the solution of the homogeneous system can be written in the form:

$$u_j^{\,c} = u_0 - \left(a\varphi_0 + \left(\frac{a}{6} - \frac{2k_\varphi}{ka} \right)\overline{C}_2 \right)j - \frac{a}{2}\overline{C}_1 j^2 - \frac{a}{3}\overline{C}_2 j^3, \quad \varphi_j^{\,c} = \varphi_0 + \overline{C}_1 j + \overline{C}_2 j^2, \tag{2.30}$$

where $\overline{C}_1$ and $\overline{C}_2$ can be obtained from the boundary conditions at the other end, j=N.

After eliminating u_i from the system (2.29), it can be shown that the particular solution of (2.3) for the rotations satisfies the equation

$$\Delta^3 \varphi_i = -\frac{aq}{k_\varphi}, \quad \Delta = f(x+1) - f(x). \tag{2.31}$$

A particular solution of the equation (2.31) can be written in the form:

$$\varphi_i^{\,p} = -\frac{aq}{k_\varphi}\frac{1}{6}i^3. \tag{2.32}$$

Then a particular solution in displacements can be found as a solution of the equation

$$\Delta^2 u_i = -\frac{a}{2}\Delta(\Delta + 2)\varphi_i - \frac{q}{k}. \tag{2.33}$$

Eventually, the particular solution of the equation (2.33) can be written in the form:

$$u_i^{\,p} = \frac{a^2 q}{24k_\varphi}i^4 + \left(\frac{a^2 q}{24k_\varphi} - \frac{q}{2k} \right)i^2. \tag{2.34}$$

Then the full solution becomes

$$u_j = u_0 - (a\varphi_0 + 2\frac{k(a^2/4) - 3k_\varphi}{3ka}\overline{C}_2)j - \frac{a}{2}\overline{C}_1 j^2 - \frac{a}{3}\overline{C}_2 j^3 + \frac{a^2 q}{24k_\varphi}j^4 + \left(\frac{a^2 q}{24k_\varphi} - \frac{q}{2k} \right)j^2, \tag{2.35_1}$$

$$\varphi_j = \varphi_0 + \overline{C}_1 j + \overline{C}_2 j^2 - \frac{aq}{6k_\varphi}j^3. \tag{2.35_2}$$

2.6.2 Non-local Cosserat continuum model of the duct/Solution of the equations of equilibrium in the non-local Cosserat continuum

According to established isomorphism (section 2.4) the non-local Cosserat solution should coincide at sphere centres with the exact (discrete) solution. It is however important to see what the continuous non-local solution looks like at the points between the sphere centres. The solution of the equations of equilibrium in the non-local Cosserat continuum (2.12) in the static case with zero volume moment and a constant volume force were obtained by Pasternak and Mühlhaus [72].

Using the conventional Fourier transform one reduces the non-local "Lamé equations" (2.12) to the following system of equations:

$$4k\sin\frac{\omega a}{2}\delta_K^{\ F}\left[\sin\frac{\omega a}{2}\overline{u}(\omega)-i\frac{a}{2}\cos\frac{\omega a}{2}\overline{\varphi}(\omega)\right]=2\pi q\delta(\omega),\tag{2.36_1}$$

$$\delta_K^{\ F}\left[ik\frac{a}{2}\sin\frac{\omega a}{2}\cos\frac{\omega a}{2}\overline{u}(\omega)+\left(k\frac{a^2}{4}\cos^2\frac{\omega a}{2}+k_\varphi\sin^2\frac{\omega a}{2}\right)\overline{\varphi}(\omega)\right]=0,\tag{2.36_2}$$

$$\delta_K^{\ F}(\omega)=\int\limits_{-\infty}^{+\infty}\delta_K(x)e^{-ix\omega}dx,\quad\overline{u}(\omega)=\int\limits_{-\infty}^{+\infty}u(x)e^{-ix\omega}dx,\quad\overline{\varphi}(\omega)=\int\limits_{-\infty}^{+\infty}\varphi(x)e^{-ix\omega}dx,\tag{2.37}$$

$\delta(\omega)$ is the ordinary Dirac-delta function.

The inverse transforms are:

$$\delta_K(x)=\frac{1}{2\pi}\int\limits_{-\infty}^{+\infty}\delta_K^{\ F}(\omega)e^{ix\omega}d\omega,\quad u(x)=\frac{1}{2\pi}\int\limits_{-\infty}^{+\infty}\overline{u}(\omega)e^{ix\omega}d\omega,\quad\varphi(x)=\frac{1}{2\pi}\int\limits_{-\infty}^{+\infty}\overline{\varphi}(\omega)e^{ix\omega}d\omega,\tag{2.38}$$

The Fourier transform of the Kunin-delta function is:

$$\delta_K^{\ F}(\omega)=\begin{cases}1,&|\omega|<\pi/a\\0,&|\omega|>\pi/a\end{cases}.\tag{2.39}$$

Correspondingly, we will look for solution of (2.36) for $|\omega|<\pi/a$. As usual, the full solution of the system (2.36) can be written in the form:

$$\overline{u}=\overline{u}^{\,c}+\overline{u}^{\,p},\ \overline{\varphi}=\overline{\varphi}^{\,c}+\overline{\varphi}^{\,p},\tag{2.40}$$

where the pair $(\overline{u}^{\,c},\overline{\varphi}^{\,c})$ is the homogeneous solution and $(\overline{u}^{\,p},\overline{\varphi}^{\,p})$ is a particular solution of the non-homogeneous system.

The determinant of the homogeneous system is equal to $k_\varphi \sin^4 \dfrac{\omega a}{2}$ and in the interval $|\omega| < \pi/a$ has a root $\omega = 0$ of the fourth order. Hence, the homogeneous solution has to be sought in the form:

$$X_j(\omega) = 2\pi C_0{}^j \delta(\omega) + 2\pi C_1{}^j \frac{\delta(\omega)}{i\omega} + 2\pi C_2{}^j \frac{2\delta(\omega)}{-\omega^2} + 2\pi C_3{}^j \frac{6\delta(\omega)}{-i\omega^3}, \quad (j=1,2), \tag{2.41}$$

where

$$X_1(\omega) = \overline{u}(\omega), \quad X_2(\omega) = \overline{\varphi}(\omega). \tag{2.42}$$

Insertion of (2.41) into the homogeneous system gives the following relations between the constants

$$C_2{}^1 = -\frac{1}{2}C_1{}^2, \; C_3{}^1 = -\frac{1}{3}C_2{}^2, \; C_3{}^2 = 0, \; C_1{}^1 = -\frac{a^2}{6}C_2{}^2 - C_0{}^2 + 2\frac{k_\varphi}{k}C_2{}^2. \tag{2.43}$$

Assuming u at $x=0$ to be u_0 and φ at $x=0$ to be φ_0 one has $C_0{}^1 = u_0$ and $C_0{}^2 = \varphi_0$. Finally, the homogeneous solution can be written in the form:

$$u^c(x) = u_0 - \left(a\varphi_0 + 2\frac{k(a^2/4) - 3k_\varphi}{3ka}\overline{C}_2\right)\frac{x}{a} - \frac{a}{2}\overline{C}_1\frac{x^2}{a^2} - \frac{a}{3}\overline{C}_2\frac{x^3}{a^3}, \tag{2.44_1}$$

$$\varphi^c(x) = \varphi_0 + \overline{C}_1\frac{x}{a} + \overline{C}_2\frac{x^2}{a^2}, \quad \overline{C}_1 = C_1{}^2 a, \quad \overline{C}_2 = C_2{}^2 a^2. \tag{2.44_2}$$

A particular solution of the system (2.36) is:

$$\overline{u}^p(\omega) = \frac{a^2\pi q}{8k_\varphi} \cdot \frac{\cos^2\dfrac{\omega a}{2}}{\sin^4\dfrac{\omega a}{2}}\delta(\omega) + \frac{\pi q}{2k}\cdot\frac{\delta(\omega)}{\sin^2\dfrac{\omega a}{2}}, \quad \overline{\varphi}^p(\omega) = -\frac{ia\pi q}{4k_\varphi}\cdot\frac{\cot\dfrac{\omega a}{2}}{\sin^2\dfrac{\omega a}{2}}\delta(\omega). \tag{2.45}$$

By performing the inverse Fourier transform and adding the homogeneous solution (2.44), full solution can be found:

$$u(x) = u_0 - \left(a\varphi_0 + \left(\frac{a}{6} - \frac{2k_\varphi}{ka}\right)\overline{C}_2\right)\frac{x}{a} - \frac{a}{2}\overline{C}_1\frac{x^2}{a^2} - \frac{a}{3}\overline{C}_2\frac{x^3}{a^3} + \left(\frac{a^2 q}{24k_\varphi} - \frac{q}{2k}\right)\frac{x^2}{a^2} + \frac{a^2 q}{24k_\varphi}\frac{x^4}{a^4} \tag{2.46_1}$$

$$\varphi(x) = \varphi_0 + \overline{C}_1\frac{x}{a} + \overline{C}_2\frac{x^2}{a^2} - \frac{aq}{6k_\varphi}\frac{x^3}{a^3}. \tag{2.46_2}$$

Alternatively, one can solve the above problem by finding the solution of the equations of motion (2.19) with zero inertia terms, in which $q(x)/(a^3\eta) = \rho g = -B$, $M(x)=0$. Then the strain and curvature can be found from the non-local constitutive relationship (2.17), (2.18) by

solving the system of two integral equations. Subsequently, the displacement and rotation fields can be obtained from (2.14).

The equations (2.19) have the following solutions:

$$\sigma(x) = Bx + \sigma(0), \quad \mu(x) = B\frac{x^2}{2} + \sigma(0)x + \mu(0), \tag{2.47}$$

where $\sigma(0)$, $\mu(0)$ are yet unknown stress and moment stress at the origin.

The solution can be rewritten in the following form:

$$u(x) = \eta[(\frac{\sigma(0)}{E} - \frac{\sigma(0)}{12E_\varphi}a^2)x - \frac{1}{2E_\varphi}\mu(0)x^2 - \frac{1}{6E_\varphi}\sigma(0)x^3 -$$

$$- \frac{B}{24E_\varphi}x^4 + \frac{B}{2E}x^2 - \frac{a^2B}{24E_\varphi}x^2] + u(0) - \varphi(0)x, \tag{2.48_1}$$

$$\varphi(x) = \frac{\eta}{E_\varphi}[\mu(0)x + \sigma(0)\frac{1}{2}x^2 + \frac{B}{6}x^3] + \varphi(0). \tag{2.48_2}$$

This form coincides with (2.46) if one sets

$$\mu(0) = \frac{k_\varphi}{\eta a^2}\overline{C_1}, \quad \sigma(0) = \frac{2k_\varphi}{\eta a^3}\overline{C_2}. \tag{2.49}$$

Using the boundary conditions $u(0)=u(L)=0$, $\varphi(0)=\varphi(L)=0$ one obtains the solution:

$$u(x) = -\frac{\eta B}{24E_\varphi}x(x-L)(x^2 + 2px + \hat{q}), \quad \varphi(x) = \frac{\eta B}{12E_\varphi}x(x-L)(2x-L), \tag{2.50}$$

$$2p = -L, \quad \hat{q} = -4\left(\frac{3E_\varphi}{E} - \frac{a^2}{4}\right), \tag{2.51}$$

and the constants $\sigma(0)$, $\mu(0)$ are:

$$\sigma_0 = \sigma(0) = -\frac{1}{2}BL, \quad \mu_0 = \mu(0) = \frac{1}{12}BL^2. \tag{2.52}$$

The normalisation

$$L = 1, \quad E = 1 \tag{2.53}$$

leads to

$$u(x) = -\frac{\eta B}{24E_\varphi}x(x-1)(x^2 + 2px + \hat{q}), \quad p = -\frac{1}{2}, \quad \hat{q} = -4(3E_\varphi - a^2/4). \tag{2.54}$$

Note that the coefficient at x^4 in (2.50_1) is positive because B is negative. This means that $u(-\infty) = u(+\infty) = +\infty$, i.e. the branches of the fourth order polynomial $u(x)$ are going

downwards at the $\pm\infty$ (the positive direction of u is directed downwards). Because of (2.54) the displacement distribution is symmetrical.

The displacement becomes zero at points:

$$x_{1,2} = \frac{1}{2}\left(1 \pm \sqrt{1+16(3E_\varphi - a^2/4)}\right). \tag{2.55}$$

If $3E_\varphi - a^2/4 > 0$, i.e. $\sqrt{3E_\varphi} > a/2$, which is the case when the rotational springs are rather stiff, then $x_1 > 1$, $x_2 < 0$. This means that both roots x_1 and x_2 are outside the duct. If $3E_\varphi - a^2/4 < 0$, i.e. $\sqrt{3E_\varphi} < a/2$, which corresponds to the case of small stiffness of the rotational springs, then $x_1 = 1-\hat{q} < 1$, $x_2 = \hat{q} > 0$. This means that both roots x_1 and x_2 are inside the duct (Figure 6). Thus, under a certain combination of constants the non-local Cosserat continuum solution exhibits a boundary effect consisting of anomalous upward displacements near the boundary.

According to (2.46$_2$), after the normalisation the rotations become (Figure 7)

$$\varphi(x) = \frac{B\eta}{12E_\varphi}x(x-1)(2x-1). \tag{2.56}$$
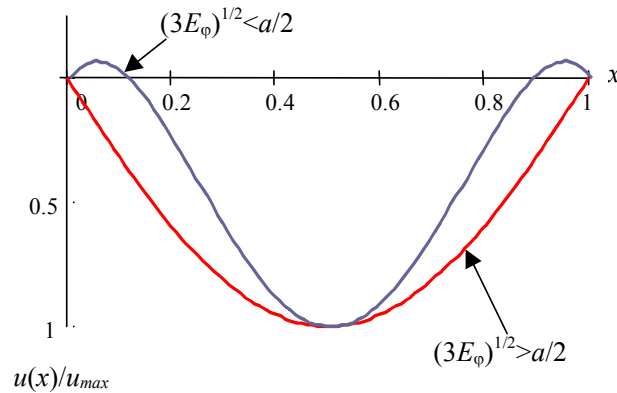

Figure 6. Distribution of normalised displacements for soft $((3E_\varphi)^{1/2}<a/2)$ and stiff $((3E_\varphi)^{1/2}>a/2)$ rotational springs.
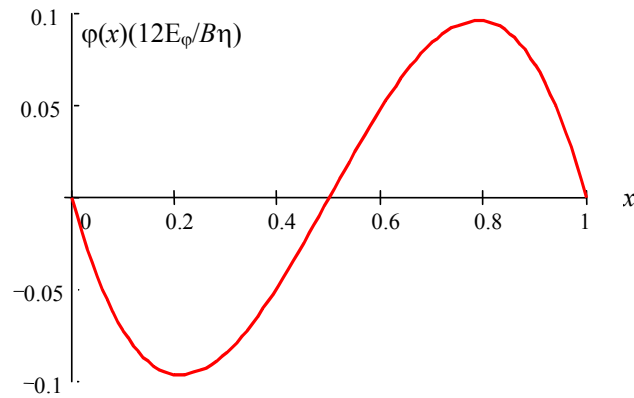
Figure 7. Distribution of normalised rotations.

2.6.3. Cosserat continuum model of the duct

Let us find the solution of the Cosserat equations of equilibrium (2.7) for the case of the constant volume force and zero volume moment ($\rho f_3 = -B$, $\rho m_2 = 0$):

$$\frac{\partial \sigma_{13}}{\partial x_1} + \rho f_3 = 0, \ \frac{\partial \mu_{12}}{\partial x_1} - \sigma_{13} = 0. \tag{2.57}$$

Denoting $-\rho f_3 = -\rho g = B$, one gets the solution of equations (2.57) in the form

$$\sigma_{13} = Bx + \sigma(0), \ \mu_{12} = B\frac{x^2}{2} + \sigma(0)x + \mu(0). \tag{2.58}$$

Then taking into account the Cosserat constitutive equations (2.6) one obtains

$$\kappa_{12} = \frac{\eta a}{k_\varphi}\left[B\frac{x^2}{2} + \sigma(0)x + \mu(0)\right], \ \gamma_{13} = \frac{\eta a}{k}[Bx + \sigma(0)]. \tag{2.59}$$

Subsequently, by using the deformation measures (2.5) rotation and displacement fields are found:

$$\varphi_2 = \frac{\eta a}{k_\varphi}\left[B\frac{x^3}{6} + \sigma(0)\frac{x^2}{2} + \mu(0)x\right] + \varphi(0), \tag{2.60}$$

$$u_3 = -\frac{\eta a}{k_\varphi}B\frac{x^4}{24} - \frac{\eta a}{k_\varphi}\sigma(0)\frac{x^3}{6} - \frac{\eta a}{k_\varphi}\mu(0)\frac{x^2}{2} + \frac{\eta a}{k}B\frac{x^2}{2} + \frac{\eta a}{k}\sigma(0)x - \varphi(0)x + u(0). \tag{2.61}$$

After satisfying the boundary conditions

$$u(0) = 0, \ u(L) = 0, \ \varphi(0) = 0, \ \varphi(L) = 0 \tag{2.62}$$

equations (2.60) and (2.61) become

$$u(x) = \frac{-\eta B}{24E_\varphi} x(x-L)(x^2 + 2px + \hat{q}^c), \quad \varphi(x) = \frac{\eta B}{12E_\varphi} x(x-L)(2x-L), \tag{2.63}$$

$$2p = -L, \quad \hat{q}^c = -12E_\varphi / E, \quad \sigma(0) = \sigma_0 = -\frac{1}{2}BL, \quad \mu(0) = \mu_0 = \frac{1}{12}BL^2. \tag{2.64}$$

Comparing the rotation fields for the Cosserat continuum model (2.63₂) with the non-local Cosserat continuum model (2.50₂), one can see that they coincide, because the constants σ_0 and μ_0 have not changed, while the displacement field (2.63₁) and (2.50₁) differ in the terms $\hat{q}$ and $\hat{q}^c$. Let us analyse this difference.

After the normalisation (2.53), the zeros of the displacement can be found:

$$x_{1,2} = \frac{1}{2}(1 \pm \sqrt{1 + 48E_\varphi}). \tag{2.65}$$

It is obvious that $1 + 48E_\varphi > 1$, therefore $x_1 > 1$, $x_2 < 0$. Both roots x_1 and x_2 are always outside the duct. This means that the boundary effects, present in the non-local Cosserat continuum model, disappear in the Cosserat model.

There has to be an explanation for that fact. The length where the boundary effect exists is defined by the value of the parameter q. Let us evaluate

$$|\hat{q}| = \left|-4(3E_\varphi - a^2 / 4)\right| < a^2.$$

Hence, the characteristic size where the boundary effect exists is of the order a^2. However, the Cosserat theory does not see the lengths lesser than a ($a^2 < a \ll 1$), the characteristic parameter of length which has been used when finite differences were replaced by the partial derivatives. That is why these boundary effects are left invisible in the Cosserat theory. Furthermore, in terms of the original discrete system, no distance smaller than a exists (there are no spheres at such distances). Therefore, the "high resolution" boundary effect is an artefact of the non-local Cosserat continuum resulting from the type of interpolation adopted.

2.6.4. Comparison of the exact solution with the solution in the non-local Cosserat and Cosserat continua

Assuming $x = ja$ one has the Cosserat solution (2.60), (2.61)

$$u_3(ja) = u_0 - \left(a\varphi(0) - \frac{2k_\varphi}{ka}\overline{C}_2\right)j - \frac{a}{2}\overline{C}_1 j^2 - \frac{q}{2k}j^2 - \frac{a}{3}\overline{C}_2 j^3 + \frac{qa^2}{24k_\varphi}j^4, \tag{2.66}$$

$$\varphi_2(ja) = \varphi_0 + \overline{C}_1 j + \overline{C}_2 j^2 - \frac{aq}{6k_\varphi} j^3,$$

(2.67)

where

$$\mu(0) = \frac{k_\varphi}{\eta a^2} \overline{C}_1, \;\; \sigma(0) = \frac{2k_\varphi}{\eta a^3} \overline{C}_2, \;\; \eta a^3 B = -q.$$

(2.68)

Comparing the Cosserat theory solution (2.66), (2.67) with the exact solution (2.35) one can conclude that rotation fields coincide completely, while the displacements differ in terms

$$-\frac{a}{6}\overline{C}_2 j \;\; \text{and} \;\; \frac{a^2 q}{24 k_\varphi} j^2.$$

If we put *ja=x* in the non-local Cosserat solution (2.46) we immediately see that the non-local Cosserat solution (2.46) coincides completely with the exact one (2.35). It means that the non-local Cosserat solution gives the exact solution at nodes where the centroids are; as we anticipated above, the result is due to the homogenisation by integral transformation. However, being a continuum solution the non-local Cosserat solution also gives some values in between nodes due to the interpolating nature of the homogenisation by integral transformation.

Figure 8a shows the comparison of the discrete (exact), non-local Cosserat and the Cosserat models solutions for a simple case of three balls. Figure 8b shows the configuration before and after the deformation.

In the above we developed two continuum models of the discrete model using two different homogenisation strategies: by differential expansions and integral transformations and compared them against the exact solution of the discrete model. The first approach led to the Cosserat continuum theory. The boundary value problem is reduced to solving the relatively simple system of two differential equations. The analysis above shows that the Cosserat continuum model of granulates gives both quite good accuracy and relative simplicity of solving the governing equations. The second approach led to the non-local Cosserat continuum theory that gave us the exact solution. The problem is reduced to solving the system of two integral equations which is more complicated than solving the system of differential equations (the first model) and in essence is no simpler than to solve the governing equations of the discrete model, the system of finite difference equations. Thus, the second homogenisation approach indeed gave us the continuum description of the discrete system, non-local Cosserat continuum. However, being just an equivalent description of the

discrete model, giving the exact solution, does not offer any simplification, which generally continuum theories are supposed to do.
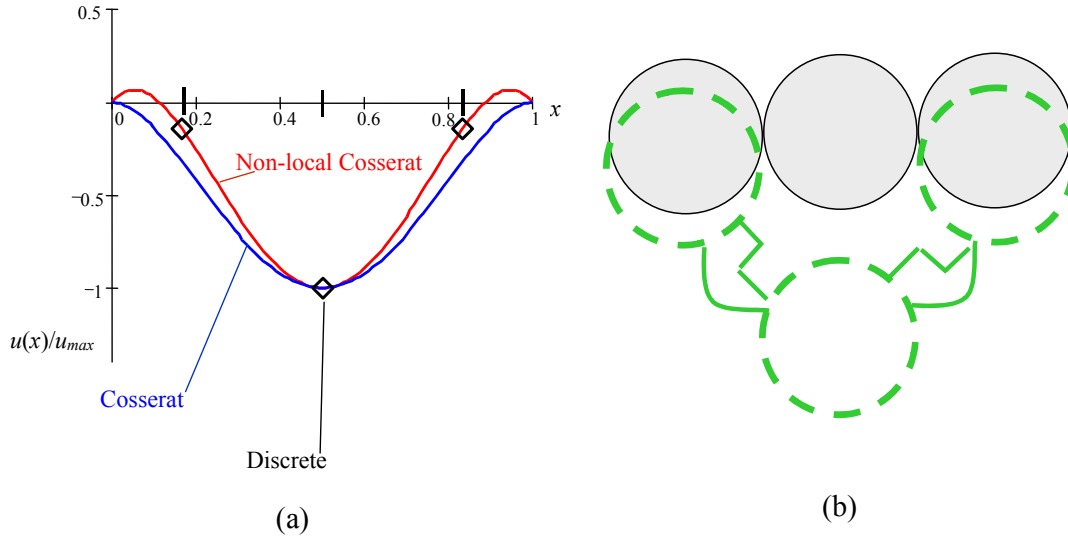

Figure 8. The comparison of the exact, non-local Cosserat and Cosserat solutions: (a) displacement distribution; diamonds indicate the centroids of the spheres; (b) configuration before (solid line) and after (broken line) the deformation in the vertical duct with three spheres.

3. WAVE PROPAGATION. DISPERSION RELATIONSHIPS

For a particular case of $q_3(x_1)=M_2(x_1)=0$ we consider the propagation of harmonic waves

$$u = Ae^{i\xi(x-v_p t)}, \quad \varphi = Be^{i\xi(x-v_p t)}, \tag{3.1}$$

where ξ is the wave number, v_p is the phase velocity. For the sake of simplicity x will be written instead of x_1, u instead of u_3 and φ instead of φ_2.

Propagation of these waves will be studied for the original physical model (2.3) and then for the Cosserat (2.8) and non-local Cosserat (2.12) models.

3.1. Wave propagation in the discrete (physical) model

By substituting (3.1) into the governing equations of the original physical model, namely the discrete equations of motion (2.3) or their homogenised (continuous) analogue (2.9), we

obtain the following system:

$$- m\xi^2 v_p{}^2 A + 4k \sin^2\left(\frac{\xi a}{2}\right) A - ika \sin(\xi a)B = 0 \,, \tag{3.2$_1$}$$

$$- J\xi^2 v_p{}^2 B + ika \sin(\xi a)A + ka^2 \cos^2\left(\frac{\xi a}{2}\right) B + 4k_\varphi \sin^2\left(\frac{\xi a}{2}\right) B = 0 \,. \tag{3.2$_2$}$$

The characteristic equation is biquadratic with respect to the phase velocity

$$mJ v_p{}^4 - 4\left(Jk \sin^2\left(\frac{\xi a}{2}\right) + \frac{1}{4} mka^2 \cos^2\left(\frac{\xi a}{2}\right) + mk_\varphi \sin^2\left(\frac{\xi a}{2}\right) \right)\frac{v_p{}^2}{\xi^2} + 16 kk_\varphi \sin^4\left(\frac{\xi a}{2}\right)\frac{1}{\xi^4} = 0 \,. \tag{3.3}$$

This equation has positive discriminant. Two real solutions of the equation give the phase velocity. Since $\forall k, k_\varphi, r, a, m, \xi$

$$mJ > 0 \,, \quad 16 kk_\varphi \sin^4\left(\frac{\xi a}{2}\right)\frac{1}{\xi^4} > 0 \,,$$

$$-4\left(Jk \sin^2\left(\frac{\xi a}{2}\right) + \frac{1}{4} mka^2 \cos^2\left(\frac{\xi a}{2}\right) + mk_\varphi \sin^2\left(\frac{\xi a}{2}\right) \right)\frac{1}{\xi^2} < 0 \,,$$

both solutions for $v_p{}^2$ are always positive. They read

$$v_p{}^2 = \frac{2k}{J\xi^2}\left[\left(\frac{2r^2}{5} + \frac{k_\varphi}{k} \right)\sin^2\left(\frac{\xi a}{2}\right) + \frac{1}{4} a^2 \cos^2\left(\frac{\xi a}{2}\right) \pm \right. \tag{3.4}$$

$$\left. \pm \sqrt{\left(\frac{k_\varphi}{k} - \frac{2r^2}{5} \right)^2 \sin^4\left(\frac{\xi a}{2}\right) + \frac{1}{16} a^4 \cos^4\left(\frac{\xi a}{2}\right) + \frac{1}{2} a^2 \left(\frac{2r^2}{5} + \frac{k_\varphi}{k} \right)\sin^2\left(\frac{\xi a}{2}\right)\cos^2\left(\frac{\xi a}{2}\right) } \right].$$

Let $r = a/2$. One can find the ratio of their amplitudes, for example from the equation (3.2$_1$):

$$\frac{A}{B} = ika \frac{\sin(\xi a)}{4k \sin^2\left(\frac{\xi a}{2}\right) - m\xi^2 v_p{}^2} \,, \tag{3.5}$$

where $v_p{}^2$ is given by (3.4).

The first type of wave (positive sign before the radical (3.4)) and the second (negative sign) have the following long wave asymptotics

$$v_p \underset{\xi \to 0}{\sim} \begin{cases} \xi^{-1} \\ \xi \end{cases}. \tag{3.6}$$

This is asymptotics of the same type as obtained by Mühlhaus and Oka [35].

The corresponding asymptotics for the ratio of amplitudes is:

$$\frac{A}{B} \underset{\xi \to 0}{\sim} \begin{cases} 0 \Rightarrow A \sim 0 & (\textit{rotational wave}) \\ \infty \Rightarrow B \sim 0 & (\textit{shear wave}) \end{cases} . \tag{3.7}$$

Thus, we have two types of waves. The first one becomes the rotational wave in the long wave limit ($\xi \to 0$), while the second one is the shear wave. Otherwise, both components are present, but asymptotically one type dominates. For that reason we will call these waves rotational-shear and shear-rotational. One should avoid considering the limiting case of $\xi \to \infty$ (short length wave) since this case cannot be described properly in terms of the physical model. This is because for large wave numbers, the ball microstructure should be taken into account and the model should be changed accordingly.

The ratio of amplitudes for different ratios of spring stiffnesses is shown in Figure 9. All the plots are given for the physically reasonable wave lengths. This is due to the fact that in the considered system the wave length cannot be shorter than the ball size. Moreover, in the homogeneous models the wave length should be much greater than the ball size.

The square of the phase velocity for rotational-shear and shear-rotational waves for different ratios of stiffnesses is shown in Figure 10.
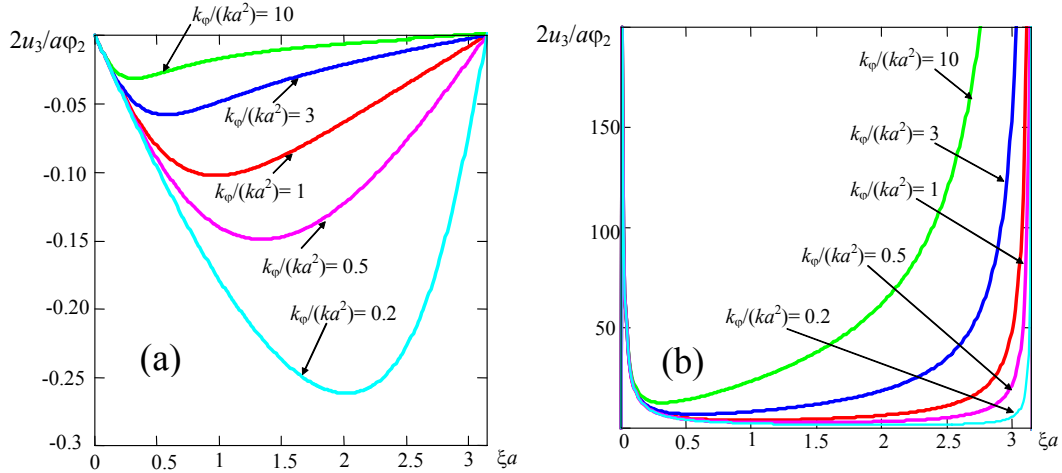

Figure 9. The ratio of amplitudes for rotational-shear (a) and shear-rotational wave (b).

3.2. Non-local Cosserat continuum

Substituting (3.1) into the non-local (integral) equations of motion (2.12$_1$)-(2.12$_2$) and calculating the corresponding integrals one can get the same system as obtained for the exact equation of motion (3.2), but with a restriction: $\xi < \pi/a$. (It does not appear mathematically for the exact solution.) This restriction reflects the fact that wave lengths must be larger than the

micro-structure size. This seems reasonable since our model was not designed to "see" something less that the microstructure size.
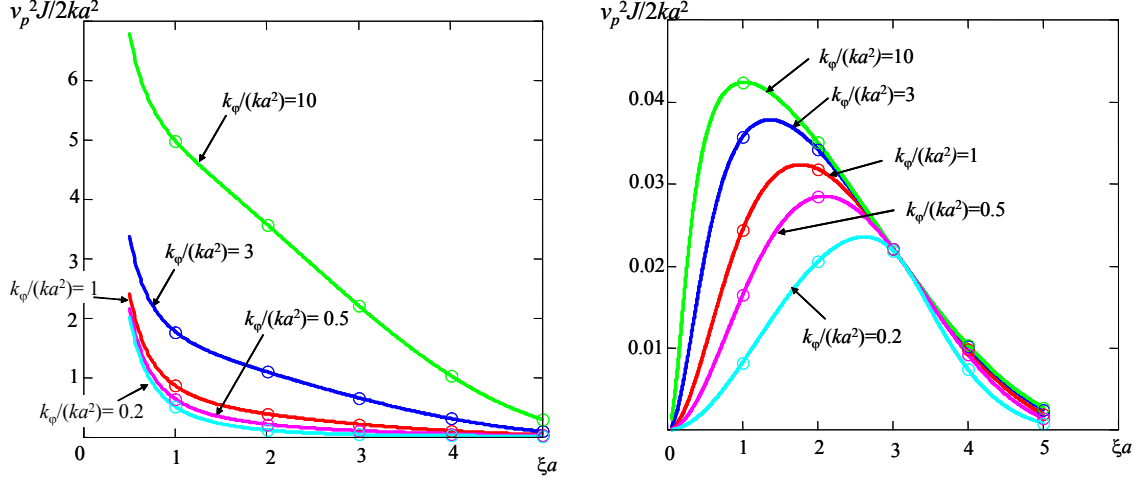

Figure 10. The square of the phase velocity for rotational-shear (a) and shear-rotational wave (b). The circles show velocities corresponding to integer values of the normalised wave number.

3.3. Cosserat continuum approximation

By assuming $f_3 = m_2 = 0$ the equations of motion (2.8_1)-(2.8_2) can be written in the form:

$$ka^2\left[\frac{\partial^2 u_3}{\partial x_1^{\,2}} + \frac{\partial \varphi_2}{\partial x_1}\right] = m\ddot{u}_3, \quad m = \rho a^3 \eta, \tag{3.8_1}$$

$$a^2\left[k_\varphi \frac{\partial^2 \varphi_2}{\partial x_1^{\,2}} - k\frac{\partial u_3}{\partial x_1} - k\varphi_2\right] = J\ddot{\varphi}_2. \tag{3.8_2}$$

Substituting (3.1) into the equations of motion one can get:

$$\frac{m}{a^2}\xi^2 v_p^{\,2} A - k\xi^2 A + i\xi kB = 0, \tag{3.9_1}$$

$$\frac{J}{a^2}\xi^2 v_p^{\,2} B - k_\varphi \xi^2 B - i\xi kA - kB = 0. \tag{3.9_2}$$

The system has the following biquadratic characteristic equation with respect to the phase velocity

$$\frac{mJ}{a^4}v_p{}^4 - \frac{1}{a^2}\left(mk_\varphi + Jk + \frac{mk}{\xi^2}\right)v_p{}^2 + kk_\varphi = 0 . \tag{3.10}$$

The discriminant is positive. Two real solutions of the equation give the phase velocity. Since $\forall k, k_\varphi, r, a, m, \xi$

$$\frac{mJ}{a^4} > 0 , \quad -\frac{1}{a^2}\left(mk_\varphi + Jk + \frac{mk}{\xi^2}\right) < 0 , \quad kk_\varphi > 0$$

both solutions for $v_p{}^2$ are always positive. They read

$$v_p{}^2 = \frac{a^2 k}{2J}\left[\left(\frac{2r^2}{5} + \frac{k_\varphi}{k}\right) + \frac{1}{\xi^2} \pm \sqrt{\left(\frac{k_\varphi}{k} - \frac{2r^2}{5}\right)^2 + \frac{1}{\xi^4} + \frac{2}{\xi^2}\left(\frac{2r^2}{5} + \frac{k_\varphi}{k}\right)}\right] . \tag{3.11}$$

This expression is an asymptotics of (3.4) as $\xi \to 0$ with the accuracy $o(\xi)$. This is not surprising since the Cosserat model is a long wave (small wave number) approximation.

   Figure 11 shows the square of the phase velocity for both rotational-shear and shear-rotational waves comparing the exact and the Cosserat solutions. They are in quite a good agreement for the small wave numbers, ie in the range where the Cosserat approximates properly the exact solution.
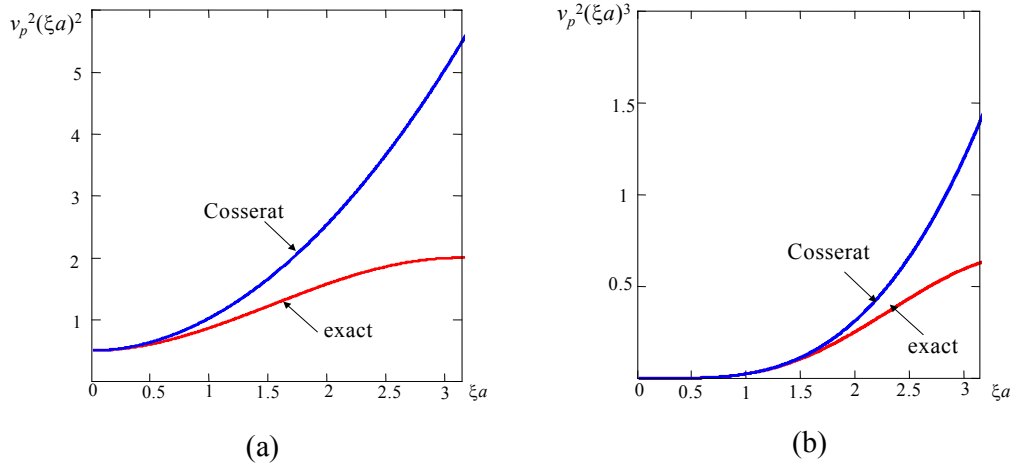

Figure 11. Comparison of the square of the phase velocity for the exact and the Cosserat solutions: (a) rotational-shear wave, (b) shear-rotational wave.

The obtained result (3.11) allows us to investigate the effect of the presence of rotational degree of freedom. Towards this end consider an asymptotics of $k_\varphi/(ka^2) \ggg 1$ which is the case when the rotations are almost suppressed. Then assuming $r = a/2$

$$v_{p1}{}^2 \sim \frac{ka^2}{J}\left[\frac{k_\varphi}{k} + \xi^{-2}\right], \quad v_{p2}{}^2 \sim \frac{0.1ka^4}{J}\left[1 - \frac{k}{k_\varphi}\xi^{-2}\right].$$ (3.12)

When the rotations are completely suppressed ($k_\varphi/(ka^2) \to \infty$), velocity of the first, rotational-shear, wave tends to infinity, but the amplitude of the displacement oscillations vanishes. The velocity of the second, shear-rotational, wave becomes

$$v_{p2_\infty} \sim a^2\sqrt{0.1k/J}\,.$$ (3.13)

This corresponds to a conventional shear wave.

In general, when $k_\varphi/(ka^2)$ is finite, the shear-rotational wave is slower than the conventional shear wave, while the rotational-shear wave is faster than the latter. When experimental measurements of wave velocities are conducted by registering the time of first arrival, one can expect that this rotational-shear wave will be registered first. This will lead to the measured wave velocity being higher than predicted by the classical elasticity, thus paving the way to experimental observation of the Cosserat effects.

4. CONCLUSIONS

In many cases it is advantageous to model real materials with internal microstructure as continua based on the well-developed machinery of modern continuum mechanics. This can be accomplished by associating each point of the continuum with a volume element, which on the one hand is large compared to the dimensions of the microstructure but on the other hand must be small as compared to the characteristic dimensions of the phenomenon to be modelled. The presence of microstructure implies that at least in principle relative movements between the microstructure and the average macroscopic deformations are possible. The relative movements may be considered by means of additional degrees of freedom. The introduction of additional degrees of freedom leads to non-classical continua, the simplest being the Cosserat continuum each point of which possesses both translational and rotational degrees of freedom. Proceeding with further degrees of freedom, one obtains higher order continua and attains more accuracy in the modelling.

The treatment of a representative volume element as a point of the macroscopic continuum imposes a restriction on the scale of the modelling: details smaller than the representative volume element are beyond the resolution of the model. It is generally believed that this restriction can be overcome by incorporating non-local constitutive laws, where, for instance, the stress at a point depends in an integral sense on the strains within a volume surrounding the point. For that reason, non-local continua do not obey the Cauchy-Euler principle: the stress state of a volume is not completely determined by the stresses at its boundary. This makes it impossible to deduce the continuum equations of motion from first principles forcing one to either hypothesise on them or to infer them from microstructural considerations.

The introduction of a suitable continuum theory to model a material with a given microstructure requires an appropriate choice of homogenisation procedure. In order to analyse different homogenisation methods we considered a model system consisting of decoupled periodic 1D chains of solid spheres connected by translational and rotational springs. The model is simple enough to allow complete analytical solutions for both static equilibrium and wave propagation. Two homogenisation techniques were considered: (1) homogenisation by differential expansion and (2) homogenisation by integral transformation (Kunin-type homogenisation). The first technique leads to a local Cosserat continuum, while the second approach gives rise to a non-local Cosserat continuum theory. The former result offered a robust balance between accuracy and simplicity being a long wave asymptotic approximation to the exact model. The second technique resulted in a non-local continuum description that yielded an exact solution, but at the same time did not really provide any simplification as compared to the exact, discrete model. In fact, there is isomorphism between the discrete model and a non-local Cosserat continuum. Interestingly, the equations of motion derived for this case using the Kunin-type homogenisation of the discrete equations assumed after the introduction of invariant deformation measures, the form expected for a Cosserat continuum. Another feature of this method is that the non-local and the discrete solutions for 1D granulates coincide at the centers of the balls. However, between the discrete points the Kunin-type homogenisation may lead to unrealistic patterns. In particular, the considered non-local model for a vertical duct under gravity showed near boundary displacements directed upwards, ie against gravity. These boundary effects are, however, limited to distances smaller than the spacing between the particle centres and are simply artefacts of the homogenisation procedure.

Homogenisation by means of integral transformation produces non-local integral relations with oscillating kernels. This oscillation is, however, not a direct consequence of the strict

periodicity of the model system. For instance, randomisation of the spring stiffnesses makes the kernels random functions with periodic means.

The analysis of wave propagation in this model system showed that two types of waves exist simultaneously: shear-rotational and rotational-shear waves, the latter being the faster ones. As the wave number tends to zero (long wavelength limit), the shear component is predominant in the shear-rotational wave, while the rotational component is predominant in the rotational-shear wave. Further analysis of the Cosserat model showed that in the limit of infinite rotational stiffness (when particle rotation is suppressed) the rotational-shear wave disappears, while the velocity of the shear-rotational wave becomes independent of the frequency indicating the absence of dispersion. The rotational-shear wave was found to be faster than the conventional shear wave. Therefore, when experimental measurements of wave velocities are conducted by registering the time of first arrival, one can expect that this rotational-shear wave will be registered first. This will lead to the measured wave velocity being higher than predicted by the classical elasticity, thus providing grounds for the experimental detection of Cosserat effects.

In conclusion, the framework of the Cosserat continuum theory was found to provide accurate descriptions of materials with microstructure. The Cosserat effects are responsible for the increase in measured wave velocities in granular materials as compared to the classical calculations that ignore rotational degrees of freedom.

REFERENCES

1. Cosserat, E. and Cosserat, F. *Théorie des corps déformables*. A. Herrmann et Fils, Paris (1909).
2. Nowacki, W. *Theory of Micropolar Elasticity*, Springer, Wien (1970).
3. Mindlin, R.D. Micro-structure in linear elasticity, *Arch. Ration. Mech. Anal.*, 16 (1964) 51-78.
4. Dyskin, A.V., Salganik, R.L. and Ustinov, K.B. Multi-scale geomechanical modelling, In: *Proc. of Western Australian Conference of Mining Geomechanics,* Kalgoorlie, Western Australia, (Szwedziki, T., Baird G.R. and Little, T.N., Eds.), Curtin University, WASM (1992) 235-246.

5. Germanivich, L.N. and Dyskin, A.V. Virial expansions in problems of effective characteristics. Part I. General concepts, *J. Mechanics of Composite Materials*, 30(2) (1994) 222-237.

6. Mühlhaus, H.-B., Dyskin, A., Pasternak, E. and Adhikary D. Non-standard continuum theories in geomechanics: theory, experiments and analysis, In: *Proc. Fourth International Conference on Constitutive Laws for Engineering Materials*, (Picu, R. C. and Kremple, E., Eds.), Troy, New York, July 27-30 (1999) 321-324.

7. Mindlin, R.D. and Tiersten, H.F. Effects of couple-stresses in linear elasticity, *Arch. Ration. Mech. Anal.*, 11 (1962) 415-448.

8. Eringen, A.C. Linear theory of micropolar elasticity, *J. Math. Mech.*, 15 (1966) 909-923.

9. Eringen, A.C. and Kafadar, C.B. Polar field theories, In: *Continuum Physics*, Volume IV, Part I, (Eringen, A.C., Ed.), Academic Press, New York (1976) 4-73.

10. Germain, P. La méthode des puissances virtuelles en mécanique des milieux continues. Première partie. Théorie du second gradient, *Journal de Mécanique*, 12 (2) (1973) 235-274.

11. Germain, P. The method of virtual power in continuum mechanics. Part 2: Microstructure, *SIAM J. Appl. Math.*, 25(3) (1973) 556-575.

12. Maugin, G.A. The method of virtual power in continuum mechanics: Application to coupled fields, *Acta Mechanica*, 35 (1980) 1-70.

13. Kunin, I.A. *Elastic media with microstructure 1. One-dimensional models*, Springer-Verlag, Berlin, Heidelberg, New-York (1982).

14. Kröner, E. The problem of non-locality in the mechanics of solids: review of the present status, In: *Fundamental Aspects of Dislocation Theory*, (Simmons, J.A., Wit, R. de and Bullough, R., Eds.), National Bureau of Standards Special Publication 317, Vol. II (1970) 729-736.

15. Kröner, E. and Datta, B.K. Non-local theory of elasticity for a finite inhomogeneous medium – A derivation from lattice theory, In: *Fundamental Aspects of Dislocation Theory*, (Simmons, J.A., Wit, R. de and Bullough, R., Eds.), National Bureau of Standards Special Publication 317, Vol. II (1970) 737-746.

16. Kunin, I.A. and Waisman, A.M. On problems of the non-local theory of elasticity, In: *Fundamental Aspects of Dislocation Theory*, (Simmons, J.A., Wit, R. de and Bullough, R., Eds.), National Bureau of Standards Special Publication 317, Vol. II (1970) 747-759.

17. Kunin, I.A. *Elastic media with microstructure I1. Three-dimensional models*, Springer-Verlag, Berlin, Heidelberg, New-York (1983).

18. Eringen, A.C. Non-local continuum description of lattice dynamics and application, In: *Constitutive Models of Deformation*, (Chandra, J. and Srivastav, R.P., Eds.), SIAM, Philadelphia (1987) 59-80.

19. Eringen, A.C. Non-local polar field theories, In: *Continuum Physics*, Volume IV, Part III, (Eringen, A.C., Ed.), Academic Press, New York (1976) 205-264.

20. Eringen, A.C. Non-local continuum mechanics and some application, In: *Non-linear Equations in Physics and Mathematics*, (Barut, A.O., Ed.), D. Reidel Publishing Company, Dordrecht, Holland (1978) 271-318.

21. Borst, R. de, Benallal, A. and Peerlings, R.H.J. On gradient-enhanced damage theories, In: IUTAM *Symposium on Mechanics of Granular and Porous Materials*, (Fleck, N.A. and Cocks, A.C.F., Eds.), Kluwer Academic Publishers, Dordrech (1997) 215-226.

22. Pijaudier-Cabot, G. and Bazant, Z.P. Non-local damage theory, *J. Engng. Mech.*, 113 (1987) 1512-1533.

23. Bazant, Z.P. and Pijaudier-Cabot, G. Non-local continuum damage, localization instability and convergence, *J. Appl. Mech.*, 55 (1988) 287-293.

24. Pijaudier-Cabot, G. Non-local damage, In: *Continuum Models for Materials with Microstructure* (Mühlhaus, H.-B., Ed.), Chapter 4, John Wiley & Sons (1995) 105-143.

25. Mühlhaus, H.-B. Continuum models for layered and blocky rock. In: *Comprehensive Rock Eng.*, Invited Chapter for Vol. **II**: Analysis and Design Methods, Pergamon Press (1993) 209-230.

26. Zvolinskii, N.V. and Shkhinek, K.N. Continual model of laminar elastic medium, *Mechanics of Solids*, 19(1) (1984) 1-9.

27. Adhikary, D.P and Dyskin, A.V. A Cosserat continuum model for layered materials, *Computers and Geotechnics*, 20 (1) (1997) 15-45.

28. Mühlhaus, H.-B. A relative gradient model for laminated materials. In: *Continuum Models for Materials with Microstructure* (Mühlhaus, H.-B., Ed.), Chapter 13, John Wiley & Sons (1995) 451-482.

29. Mühlhaus, H.-B. and Hornby, P. A relative gradient theory for layered materials, *J. Phys. IV France*, 8 (1998) 269-276.

30. Mühlhaus, H.-B. and Hornby, P. A beam theory gradient continua. In: *Material*

Instabilities in solids (de Borst, R. and van der Giessen, E., Eds.), Chapter 32, John Wiley & Sons (1998) 521-532.

31. Sulem, J. and Mühlhaus, H.-B. A continuum model for periodic two-dimensional block structures, *Mechanics of Cohesive-Frictional Materials*, 2 (1997) 31-46.

32. Mühlhaus, H.-B. and Vardoulakis, I. The thickness of shear bands in granular materials, *Géotechnique*, 37 (1987) 271-283.

33. Mühlhaus, H.-B., Borst, R. de and Aifantis, E.C. Constitutive models and numerical analyses for inelastic materials with microstructure. In: *Computing Methods and Advances in Geomechanics* (Beer, G., Booker, J.R. and Carter, J., Eds.), Balkema, Rotterdam (1991) 377-385.

34. Chang, C.S. and Ma, L. Elastic material constants for isotropic granular solids with particle rotation, *Int. J. Solids Structures*, 29 (1992) 1001-1018.

35. Mühlhaus, H.-B. and Oka, F. Dispersion and wave propagation in discrete and continuous models for granular materials, *Int. J. Solids Structures*, 33 (1996) 2841-2858.

36. Mühlhaus, H.-B. and Hornby, P. On the reality of antisymmetric stresses in fast granular flows, In: *IUTAM Symposium on Mechanics of Granular and Porous Materials*, (Fleck, N.A. and Cocks, A.C.F., Eds.), Kluwer Academic Publishers, Dordrech (1997) 299-311.

37. Wells, G.N. and Sluys, L.J. Partition-of-unity for fracture of brittle materials, In: *Bifurcation and Localization in Geomechanics* (Mühlhaus, H.-B., Dyskin, A.V. and Pasternak, E., Eds.), Swets & Zeitlinger, Lisse (2001) 169-176.

38. Hill, R. Elastic properties of reinforced solids: some theoretical principles, *J. Mech. Phys. Solids*, 11 (1963) 357-372.

39. Mori, T. and Tanaka, K. Average stress in matrix and average elastic energy of materials with misfitting inclusions, *Acta Metal.*, 21 (1973) 571-574.

40. Christensen, R.M. *Mechanics of Composite Materials*, John Wiley & Sons, New York (1979).

41. Hashin, Z. The differential scheme and its application to cracked materials, *J. Mech. Phys. Solids*, 36(6) (1988) 719-734.

42. Kachanov, M. Effective elastic properties of cracked solids: critical review of some basic concepts, *Applied Mechanics Reviews*, 45(8) (1992) 304-335.

43. Nemat-Nasser, S. and Horii, H. *Micromechanics: Overall Properties of Heterogeneous Materials*. North-Holland-Amsterdam, London, New York, Tokyo

(1993).

44. Krajcinovic, D. *Damage Mechanics*, Elsevier, Amsterdam, Lausanne, New York, Oxford, Shannon, Tokyo (1996).

45. Cambou, B. Micromechanical approach in granular materials, In: *Behaviour of Granular Materials*, (Cambou, B., Ed.), CISM Courses and Lectures, No 385, Springer, Wien New York (1998) 171-216.

46. Savin, G.N. and Khoroshun, L.P. The problem of elastic constants of stoichastically reinforced materials, *Mekhanika sploshnoy sredy i rodstvennye problemy analiza* [Mechanics of continuous media and related problems of analysis], Moscow, Nauka Press (1972) 437-444 (in Russian).

47. Khoroshun, L.P. Methods of theory of random functions in problems of macroscopic properties of microinhomogeneous media, *Soviet Applied Mechanics*, 14(2) (1978) 113-124.

48. Duffy, J. and Mindlin, R.D. Stress-strain relation and vibrations of granular medium, *J. Appl. Mech.*, 24 (1957) 585-593.

49. Deresiewicz, H. Stress-strain relations for a simple model of a granular medium, *J. Appl. Mech.*, 25 (1958) 402-406.

50. Meguid, S.A. and A.L. Kalamkarov Asymptotic homogenization of elastic materials with a regular structure, *Int. J. Solids Structures*, 31(3) (1994) 303-316.

51. Vanin, G.A. *Micromechanics of Composite Materials*, Naukova Dumka, Kiev (1985) (in Russian).

52. Maugin, G. A. *Non-linear Waves in Elastic Crystals*, Oxford University Press, Oxford (1999).

53. Suiker, A.S.J., Borst, R. de and Chang, C.S. Micro-mechanically based higher-order continuum models for granular materials, In: *Constitutive Modelling of Granular Materials*, (Kolymbas, D., Ed.), Springer, Berlin (2000) 249-274.

54. Suiker, A.S.J., Borst, R. de and Chang, C.S. Micro-mechanical modelling of granular material. Part 1: Derivation of a second-gradient micro-polar constitutive theory, *Acta Mechanica*, 149 (2001) 161-180.

55. Suiker, A.S.J., Borst, R. de and Chang, C.S. Micro-mechanical modelling of granular material. Part 2: Plane wave propagation in finite media, *Acta Mechanica*, 149 (2001) 181-200.

56. Satake, M. Three-dimensional discrete mechanics of granular materials, In: *IUTAM Symposium on Mechanics of Granular and Porous Materials*, (Fleck, N.A. and Cocks,

A.C.F., Eds.), Kluwer Academic Publishers, Dordrech (1997) 193-202.

57. Tüzün, U. and Heyes, D.M. Distinct element simulations and dynamic microstructural imaging of slow shearing granular flows, In: *IUTAM Symposium on Mechanics of Granular and Porous Materials*, (Fleck, N.A. and Cocks, A.C.F., Eds.), Kluwer Academic Publishers, Dordrech (1997) 263-274.

58. Thornton, C. Microscopic approach contributions to constitutive modelling, In: *Constitutive Modelling of Granular Materials*, (Kolymbas, D., Ed.), Springer, Berlin (2000) 193-208.

59. Mühlhaus, H.-B., Moresi, L. and Sakaguchi, H. Discrete and continuum modelling of granular materials, In: *Constitutive Modelling of Granular Materials*, (Kolymbas, D., Ed.), Springer, Berlin (2000) 209-224.

60. Gudehus, G. A comprehensive constitutive equation for granular materials, In: *Soils and Foundations*, Vol. 36(1) (1996) 1-12.

61. Digby, P.J. The effective elastic moduli of porous granular rocks, *J. Appl. Mech*., **16**, 803-808 (1981).

62. Walton, K. The effective elastic modulus of a random packing of spheres, *J. Mech. Phys. Solids*, 35 (1987) 213-226.

63. Bathurst, R.J. and Rothenberg, L. Micromechanical aspects of isotropic granular assemblies with linear contact interactions, *J. Appl. Mech*., 55 (1988) 17-23.

64. Chang, C.S Micromechanical modelling of constitutive relations for granular material, In: *Micromechanics of Granular Materials*, (Satake, M. and Jenkins, J.T., Eds.), Elsevier Science Publishers B. V., Amsterdam (1988) 271-279.

65. Jenkins, J.T. Volume change in small strain axisymmetric deformations of a granular material, In: *Micromechanics of Granular Materials*, (Satake, M. and Jenkins, J.T., Eds.), Elsevier Science Publishers B. V., Amsterdam (1988) 245-252.

66. Cambou, B. Dedecker, F. and Chaze, M. Relevant local variables for the change of scale in granular materials, In: *Constitutive Modelling of Granular Materials*, (Kolymbas, D., Ed.), Springer, Berlin (2000) 275-290.

67. Fleck, N.A. and Cocks, A.C.F. (Eds.) *IUTAM Symposium on Mechanics of Granular and Porous Materials*, Kluwer Academic Publishers, Dordrech (1997).

68. Pasternak, E. and Mühlhaus, H.-B. Non-classical continua for modelling of granulate materials. In: *The 2001 ANZIAM Applied Mathematics Conference Abstracts* (Denier, J.P. and Tuck E.O., Eds.), Barossa Valley, South Australia, February 3-7 (2001) 64.

69. Pasternak, E. and Mühlhaus, H.-B. Cosserat continuum modelling of granulate

materials, In: *Computational Mechanics – New Frontiers for New Millennium* (Valliappan, S. and Khalili, N., Eds.), Elsevier Science (2001) 1189-1194.

70. Pasternak, E. and Mühlhaus, H.-B. Large deformation Cosserat continuum modelling of granulate materials, In: *Applied mechanics. Progress and application. ACAM 2002 The Third Australasian Congress on Applied Mechanics Sydney, February 20-22, 2002* (Zhang, L., Tong, L. and Gal, J., Eds.), World Scientific, Singapore, New Jersey, London, Hong Kong (2002) 389-396.

71. Pasternak, E. and Mühlhaus, H.-B. Cosserat and non-local continuum models for problems of wave propagation in fractured materials, In: *7th International Symposium on Structural Failure and Plasticity - IMPLAST2000*, (X.L. Zhao and R.H. Grzebieta, Eds.), 4-6 October 2000, Melbourne, Pergamon (2000) 741-746.

72. Pasternak, E. and Mühlhaus, H.-B. A non-local Cosserat model of heterogeneous materials: 1D structures, In: *Structural integrity and fracture* (Dyskin, A.V., Hu, X. and Sahouryeh, E., Eds.), Swets & Zeitlinger, Lisse (2002) 107-114.

73. Graff, K. F. *Wave motion in elastic solids*, Dover Publications, New York (1975).

74. Kahane, J.-P. *Some Random Series of Functions*. Second edition, Cambridge University Press, Cambridge (1985).